〔症例3(図4)〕58歳，女性．変形性膝関節症．
約3年前から，歩行時，左膝関節内側に疼痛が出現し，徐々に痛みが増強した．単純X線では，左膝内側関節裂隙の狭小化を認めた．MRIによると，内側関節軟骨は，菲薄化しているものの残存しており，年齢も考慮して，高位脛骨骨切り術を選択した．骨切り後の骨欠損部には，術前CT三次元構成画像に基づき，切削機により加工したブロック状人工骨(NEOBONE)を移植した(a～g)．術後6カ月で良好な骨癒合が得られた(h)．

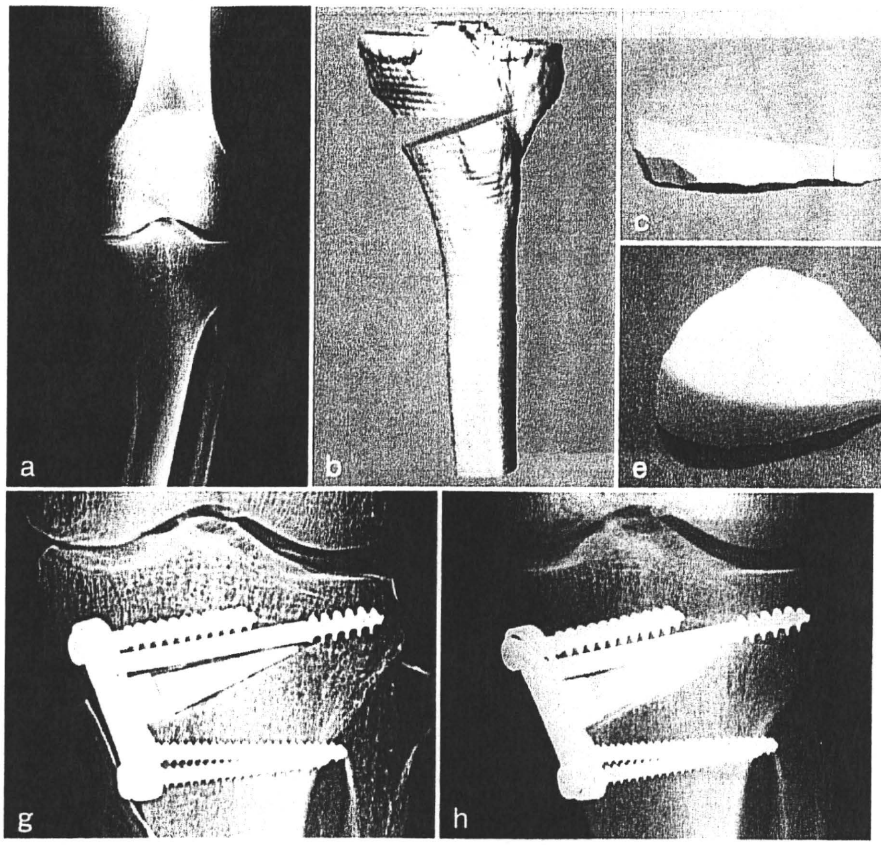

図4 左変形性膝関節症
a：術前の単純X線像，b：高位脛骨骨切り術の計画，c：骨欠損部の再構成，d：コンピュータデータによる切削加工，e：加工済み人工骨(NEOBONE)，f：術中，g：術直後の単純X線像，h：術後6カ月の単純X線像．

〔症例4(図5)〕58歳，女性．関節リウマチ．
10年前に発症した関節リウマチで治療中に右手関節の疼痛が著明となった．単純X線では，手根骨の骨破壊と橈骨関節近傍の円形の骨溶解像を認めた(a)．関節リウマチによる骨嚢胞と診断し，骨破壊の進行予防，病的骨折予防の目的で，骨嚢胞に対し人工骨移植術を施行した．橈骨骨皮質を小開窓し，嚢胞内を掻爬後，顆粒状人工骨(NEOBONE)を充填した(b・c)．術後1カ月で手関節痛は軽減し，以後徐々に骨形成が進行した(d)．術後2年，疼痛は消失している．

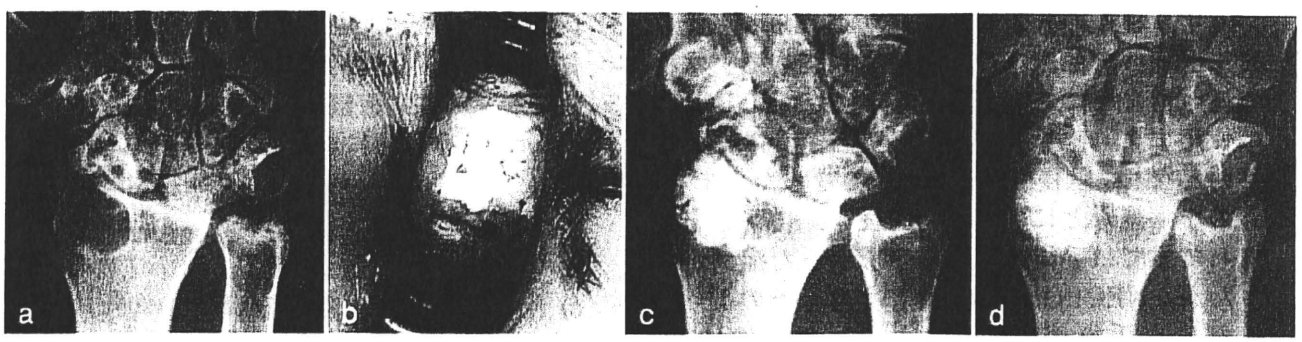

術前　　術中　　術直後　　術後12カ月

図5 右手関節の関節リウマチ

〔症例5(図6)〕65歳，女性．関節リウマチ．
7年前に発症した関節リウマチで治療中に左膝関節の疼痛が著明となった．単純X線では，膝関節の骨破壊，関節裂隙の消失，脛骨近位中央部の巨大な嚢腫様変化を認めた(a・b)．この状態での人工膝関節の設置は不安定であるため，骨破壊の進行予防，病的骨折予防の目的で，まず脛骨骨嚢胞に対し，人工骨(NEOBONE)移植術を施行した(c)．術後6カ月で，良好な骨再生が確認されたため，この時点で人工膝関節全置換術を施行した(d)．術後3年，人工関節のゆるみも生じず，経過良好である．

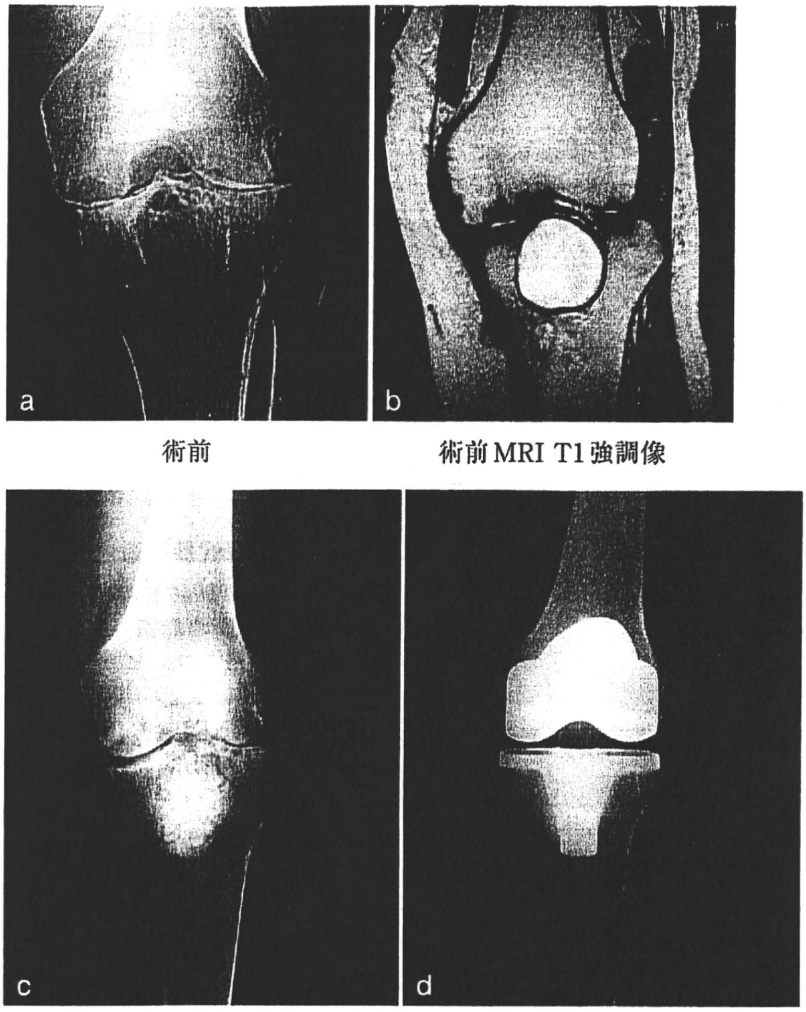

術前　　術前MRI T1強調像

術直後　　人工膝関節全置換術直後

図6　左膝関節の関節リウマチ

〔まとめ〕

近年，種々の人工骨の開発が進められ，骨の再生医療への臨床応用が期待されている．本稿で述べたように，筆者らが開発したNEOBONEの使用により，骨盤などからの自家骨の採取が不要となり，低侵襲手術が可能となった．また，骨の小病変などに対しては，従来，自家骨を採取してまでは手術適応とならなかった症例があったが，NEOBONEの使用により，そのような症例にも手術適応が拡大した．将来的には，NEOBONEの気孔間連通構造を利用して，骨髄幹細胞や骨形成蛋白(BMP)等の増殖因子を気孔内に導入したり，外科的に血管を導入することにより，さらなる骨再生の促進が期待できる．近い将来，先端医療としての骨組織のtissue engineeringが可能になるものと思われる．

〔参考文献〕

1) 吉川秀樹，他：カレントテラピー 21：276，2003.
2) 玉井宣行，他：関節外科 23：256，2004.
3) 名井　陽，他：骨・関節・靱帯 17：1205，2004.
4) 名井　陽，他：日整会誌 80：262，2006.
5) 吉川秀樹：関節外科 25：999，2006.
6) 名井　陽，他：治療 90：1815，2008.

Biochemical and Biophysical Research Communications 378 (2009) 186–191

Contents lists available at ScienceDirect

Biochemical and Biophysical Research Communications

journal homepage: www.elsevier.com/locate/ybbrc

Adenovirus-mediated gene transfer of adiponectin reduces the severity of collagen-induced arthritis in mice

Kosuke Ebina [a,b], Kazuya Oshima [a], Morihiro Matsuda [b,c,d], Atsunori Fukuhara [b], Kazuhisa Maeda [b], Shinji Kihara [b], Jun Hashimoto [a], Takahiro Ochi [e], Nirmal K. Banda [f], Hideki Yoshikawa [a], Iichiro Shimomura [a,*]

[a] Departments of Orthopaedics and Metabolic Medicine, Graduate School of Medicine, Osaka University, 2-2 Yamadaoka, Suita, Osaka 565-0871, Japan
[b] Metabolic Medicine, Graduate School of Medicine, Osaka University, 2-2 Yamadaoka, Suita, Osaka 565-0871, Japan
[c] Division of Analysis for Pathophysiology, Institute of Clinical Research, National Hospital Organization Kure Medical Center, Kure, Hiroshima 737-0023, Japan
[d] Department of Internal Medicine, National Hospital Organization Kure Medical Center, Kure, Hiroshima 737-0023, Japan
[e] Osaka Police Hospital, 10-31 Kitayama-cho, Tennoji-ku, Osaka 543-0035, Japan
[f] Division of Rheumatology B115, University of Colorado at Denver and Health Sciences Center, M-20 3104, 1775 North Ursula St., Aurora, CO 80045, USA

ARTICLE INFO

Article history:
Received 24 October 2008
Available online 21 November 2008

Keywords:
Adiponectin
Collagen-induced arthritis
Complement
Disease severity
Inflammation
Mice
Rheumatoid arthritis

ABSTRACT

Adiponectin (APN) is a hormone released by adipose tissue with anti-inflammatory properties. The purpose of this study was to examine the therapeutic effects of systemic delivery of APN in murine arthritis model. Collagen-induced arthritis (CIA) was induced in male DBA1/J mice, and adenoviral vectors encoding human APN (Ad-APN) or beta-galactosidase (Ad-β-gal) as control were injected either before or during arthritis progression. Systemic APN delivery at both time points significantly decreased clinical disease activity scores of CIA. In addition, APN treatment before arthritis progression significantly decreased histological scores of inflammation and cartilage damage, bone erosion, and mRNA levels of pro-inflammatory cytokines in the joints, without altering serum anti-collagen antibodies levels. Immunohistochemical staining showed significant inhibition of complement C1q and C3 deposition in the joints of Ad-APN infected CIA mice. These results provide novel evidence that systemic APN delivery prevents inflammation and joint destruction in murine arthritis model.

Rheumatoid arthritis (RA) is an autoimmune disease characterized by chronic inflammation of joint synovial tissues, followed by cartilage destruction and bone erosion. Collagen-induced arthritis (CIA) is an established rodent model of autoimmune polyarthritis with many similarities to human RA, and the immunopathological process of CIA has been reported in details [1]. Briefly, injection of chicken type II collagen (CII) in complete Freund's adjuvant (CFA) results in proliferation and differentiation of T-cells into CD4+Th1-cells in the draining lymph nodes. These cells then promote the production of anti-collagen IgG by activated CII-specific B-cells. These antibodies enter the joint and bind to CII, forming an immunocomplex (IC), which activates the complement cascade. Complement enhances the permeability of the vascular endothelium, and facilitates infiltration of monocytes (macrophages) and neutrophils into the joint. In the joint space, macrophages produce tumor necrosis factor (TNF)-α and interleukin (IL)-1. TNF-α enhances vascular permeability and migration of inflammatory cells into the joint space, and IL-1 is the primary trigger of tissue destruction by infiltrating cells and resident synoviocytes.

Adiponectin (APN) is an adipocytokine that shares strong homologies with the complement factor C1q and TNF-α [2]. APN has anti-inflammatory effects, and suppresses TNF-α and IL-6 production by macrophages activated with lipopolysaccharide (LPS) through suppression of nuclear factor-kappa B (NF-κB) signaling [3]. Accumulating evidence suggests a novel link between APN and inflammatory joint diseases. For example, APN concentration in the synovial fluid correlates negatively with synovial fluid leukocyte count in patients with RA, suggesting that APN is an anti-inflammatory molecule in RA [4]. However, APN levels in synovial fluid and serum are elevated in patients with RA compared with healthy controls [4], and APN treatment induces IL-6 production by synovial fibroblasts from RA patients [5], suggesting that APN is a pro-inflammatory molecule in RA. Thus, the effects of APN in RA are controversial. In the present study, we investigated the effects of APN on CIA mice using APN-producing adenovirus.

Materials and methods

Materials. Enzyme-linked immunosorbent assay (ELISA) for murine APN (including all isoforms) was purchased from Otsuka Pharmaceutical (Tokyo, Japan). Anti-APN polyclonal antibody used

* Corresponding author. Fax: +81 6 6879 3739.
E-mail address: ichi@imed2.med.osaka-u.ac.jp (I. Shimomura).

0006-291X/$ - see front matter © 2008 Elsevier Inc. All rights reserved.
doi:10.1016/j.bbrc.2008.11.005

for Western blotting was described previously [6]. Tartrate-resistant acid phosphatase (TRAP) staining kit was purchased from Cell Garage (Tokyo, Japan).

Induction and assessment of CIA. To induce CIA, we injected intradermally 100 μl of an emulsion containing 200 μg of chicken CII (Sigma, St. Louis, MO) and 200 μg of *Mycobacterium tuberculosis* in CFA (Chondrex, Redmond, WA) at the base of the tail of 6-week-old male DBA/1J mice (CLEA Japan, Tokyo), twice with a 21-day gap, as described previously [7]. Clinical severity of arthritis was assessed as described previously [8]. Each limb was scored, yielding a maximum possible score of 16 per mouse. Serum was collected from the tail vein at each time point.

APN adenovirus and systemic delivery in vivo. Adenovirus producing the full-length mouse APN was prepared as described previously [9]. Then, 200 μl of 2×10^8 plaque-forming units of adiponectin-producing adenovirus (Ad-APN) or control β-galactosidase-expressing adenovirus (Ad-β-gal) were injected into the jugular vein, on 19 (before arthritis progression) or 27 (during arthritis progression) days after initial injection of CII.

Determination of IgG, IgG2a, and IgG1 titers against CII and serum complement C1q and C3 levels. The total IgG anti-collagen antibody titers against chicken CII were determined through ELISA kit (Chondrex). IgG1 and IgG2a anti-collagen antibody titers against chicken CII were determined as described previously, and expressed in optical density (OD) value [10]. Serum C1q and C3 levels were determined by ELISA as described previously [11].

Histological analysis. On day 35 after initial injection of CII, joints were harvested and fixed in phosphate-buffered 4% paraformaldehyde, decalcified in 14% ethylenediaminetetraacetic acid (EDTA), and embedded in paraffin. Joint sections were stained with Safranin O and hematoxylin/eosin, and then histologically scored for inflammation, cartilage damage, and pannus formation as described previously [12]. Immunostaining for mouse IgG, C1q, C3, neutrophils, CXC chemokine ligand (CXCL)12, and APN was performed on paraffin-embedded samples with goat anti-mouse IgG (Cappel), rat anti-mouse C1q (Hycult Biotechnology b.v., Uden, Netherlands), rat anti-mouse C3 (Hycult Biotechnology), rat-anti-mouse neutrophils, (Serotec, Oxford, UK), monoclonal antihuman/mouse CXCL12 antibody (R&D Systems Inc., Minneapolis, MN), and rabbit-anti-mouse APN (Otsuka Pharmaceutical), respectively. The other steps were performed according to the instructions provided on the labeling of Vectastain Elite ABC system (Vector Laboratories, Burlingame, CA). Scoring for IgG, C1q and C3 staining on the cartilage, and CXCL12 staining on the synovium was performed as described previously [13]. The average number of infiltrating neutrophils in the synovium was determined using a modified version of the published method [14].

Quantitative real-time PCR of joint samples. Total RNA was extracted by pulverizing the frozen individual fore paws with an RNA STAT-60 kit. The first-strand cDNA was synthesized using ThermoScript RT-PCR System (Invitrogen, San Diego, CA). Real-time polymerase chain reaction (PCR) was performed on a Light Cycler using the Fast Start DNA Master SYBR Green I (Roche Diagnostics, Indianapolis, IN). The sequences of primers were designed based on a previous report [13], and other primers are listed in Supplementary Table 1.

Lymph node cell proliferation assay. In vitro proliferation of draining lymph node (DLN) cells was examined by Cell Proliferation ELISA Bromodeoxyuridine (BrdU) kit (Roche) using a modified version of the published method [10].

Cytokine production by cultured splenocytes. Spleens were removed and cell suspensions (2×10^6 cells/well) were distributed to flat bottom 96-well plates. Spleen cells were cultured without or with either 50 μg/ml heat-denatured chicken CII (Sigma–Aldrich) or 5 μg/ml LPS from *Escherichia coli* (Sigma–Aldrich). After 48-h incubation, the supernatants were collected, and TNF-α and IL-1β levels were measured using ELISA kit (Quantikine Mouse ELISA kit, R&D Systems Inc.).

Skeletal morphology. Three-dimensional microcomputed tomography (3D-μCT) scan for ankle joints was undertaken and the trabecular bone area (percentage of bone volume [BV] per tissue volume [TV]) of distal tibia was measured using a composite X-ray analysis system (Shimadzu, SMX-100CT-SV, Kyoto, Japan).

Statistical analysis and ethical considerations. Data were expressed as means ± standard error of the mean. Differences between groups were examined for statistical significance using Chi-square test, Student's *t* test, or analysis of variance with Fisher's protected least significant difference test. A *P* value less than 0.05 denoted the presence of a statistically significant difference. The experimental protocol was approved by the Ethics Review Committee for Animal Experimentation of Osaka University School of Medicine.

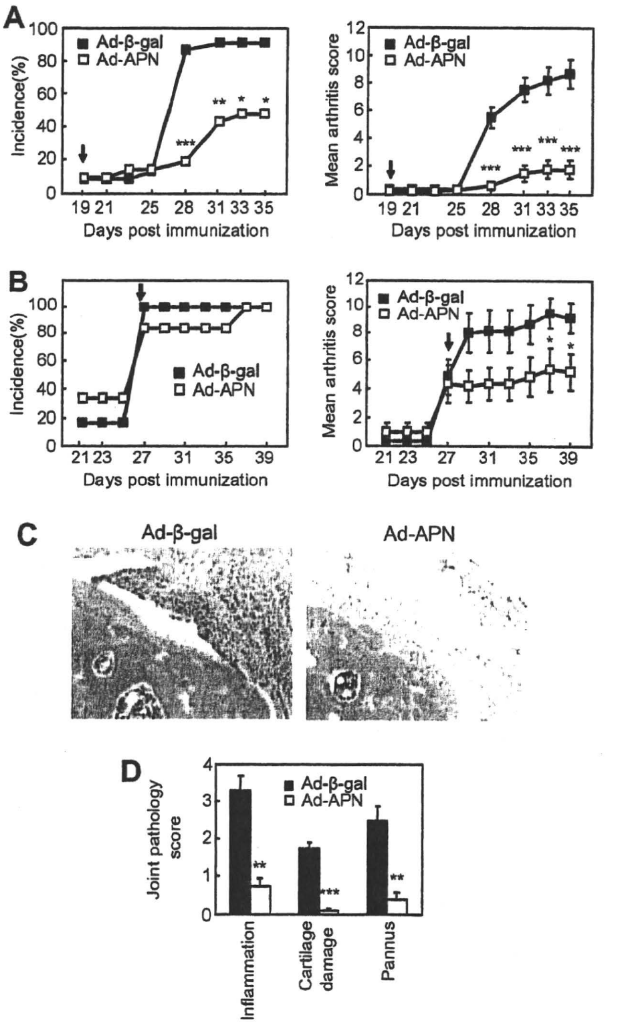

Fig. 1. Systemic delivery of APN in collagen-induced arthritis (CIA) mouse model and histological analysis of the joints. (A) On day 19, before arthritis progression, mice were injected with adenoviral vector directing the expression of either *lacZ* gene (Ad-β-gal) or APN (Ad-APN) intravenously ($n = 23$ Ad-β-gal-infected mice, $n = 21$ Ad-APN-infected mice). (B) On day 27, during arthritis progression, mice were injected with the same adenovirus (n = 6 mice in each group). (C) Histological features of representative hematoxylin and eosin-stained sections of the ankle joints (original magnification 200×), and (D) mean pathological scores of the joints of adenovirus-infected CIA mice ($n = 36$ joints in each group). $^{*}P < 0.05$, $^{**}P < 0.01$, $^{***}P < 0.001$, versus Ad-β-gal-infected CIA mice.

Results

Ad-APN suppresses progression of arthritis in CIA model

First, we tried two protocols to evaluate the effect of Ad-APN on CIA. When the virus was injected on day 19 (Fig. 1A), the incidence and disease activity on day 35 were significantly suppressed by Ad-APN treatment compared with Ad-β-gal (arthritis score: Ad-APN-infected mice: 1.76 ± 0.63, Ad-β-gal-infected mice: 8.68 ± 1.06; $P < 0.001$). In addition, when the virus was injected on day 27 (Fig. 1B), disease activity was significantly suppressed on day 39 by Ad-APN treatment compared with Ad-β-gal (arthritis score: Ad-APN-infected mice: 5.17 ± 1.25, Ad-β-gal-infected mice: 9.17 ± 1.15; $P < 0.05$). For the rest of this study, we used the former protocol (Fig. 1A). Histological analysis of the ankle joint showed typical features of active arthritis in Ad-β-gal-infected CIA mice, including infiltration of inflammatory cells into the synovium, cartilage damage, and pannus formation. These changes were significantly less pronounced in Ad-APN-infected CIA mice (Fig. 1C and D).

Ad-APN increases APN protein in serum and bone marrow, and does not alter serum anti-collagen antibodies or complement levels

In the experiments described in Fig. 1A, injection of Ad-APN resulted in about 5-fold increase on day 21 and about 30-fold increase on day 35 in serum APN levels (Fig. 2A). The high serum APN protein levels in Ad-APN-infected CIA mice were mainly composed of high- and middle-molecular weight forms of APN (Fig. 2B). Moreover, Ad-APN substantially increased APN protein content in knee joints compared with Ad-β-gal (Fig. 2C). Immunohistochemical staining of knee joints with anti-APN antibody indicated accumulation of APN in the bone marrow but not on the cartilage surface in Ad-APN-infected CIA mice (Fig. 2D). Under such conditions, anti-CII IgG, IgG2a, and IgG1 titers, serum C1q and C3 levels were not different between Ad-APN- and Ad-β-gal-infected CIA mice (Fig. 2E and F).

Treatment of CIA mice with Ad-APN suppresses local deposition of C1q and C3, infiltration of neutrophil, and changes in mRNAs of pro-inflammatory genes

Next, we examined the accumulation of IgG, C1q, and C3 on the cartilage of wrist, knee, and ankle joints by immunohistochemical staining (Fig. 3A and B). Under the conditions with minimum background staining, IgG deposition on the cartilage was observed in both adenovirus-infected CIA mice. On the other hand, C1q and C3 deposits on the cartilage were significantly suppressed by Ad-APN treatment compared with Ad-β-gal. Furthermore, neutrophil infiltration and synovium deposition of CXCL12, a chemokine that promotes leukocyte migration, were also significantly decreased in Ad-APN-infected CIA mice (Fig. 3A and B). To assess the inflammatory status, mRNA levels of pro-inflammatory genes, complement factors, and F4/80 (a marker of monocyte/macrophage linage) were measured in isolated forepaws. The expression levels of IL-1β, IL-6, COX-2 IFN-γ, TNF-α, C1q, C3, and F4/80 were all significantly decreased by Ad-APN treatment (Fig. 3C).

Effects of Ad-APN on immunocyte activities in lymph nodes and spleen, and bone erosion of CIA mice

Next, activities of immunocytes were measured. DLN cells from Ad-APN-infected CIA mice showed marginally inhibited proliferation activities (Fig. 4A). Splenocytes from Ad-APN-infected CIA

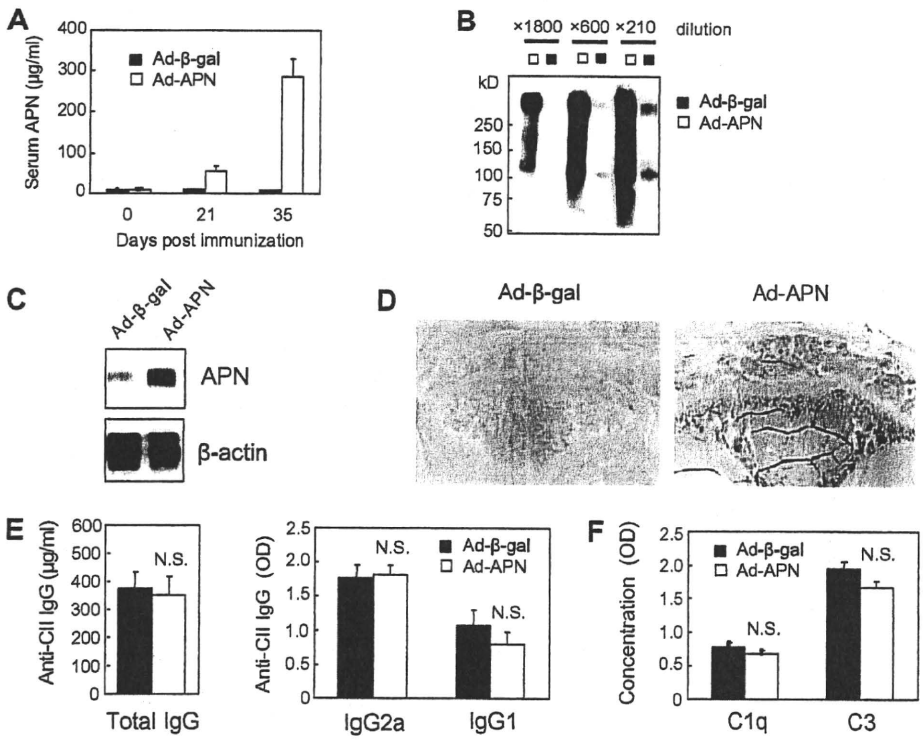

Fig. 2. High APN levels in serum and joints do not alter serum levels of anti-CII antibody, complement C1q, or C3 in CIA mice. (A) Serum APN concentrations at each time point were determined by ELISA ($n = 6$ in each group). Representative serum samples (B) and protein lysates prepared from knee joints (C) of adenovirus-infected CIA mice on day 35 were subjected sodium dodecyl sulfate-polyacrylamide gel electrophoresis without reducing reagent, and analyzed by western blot using anti-APN antibody. (D) Representative sections of proximal tibia immunostained with APN (original magnification 40×). Serum samples were obtained on day 35, and anti-CII specific IgG, IgG2a, and IgG1 levels (E), and complement C1q and C3 levels (F) were measured by ELISA ($n = 6$ in each group). NS = not significant.

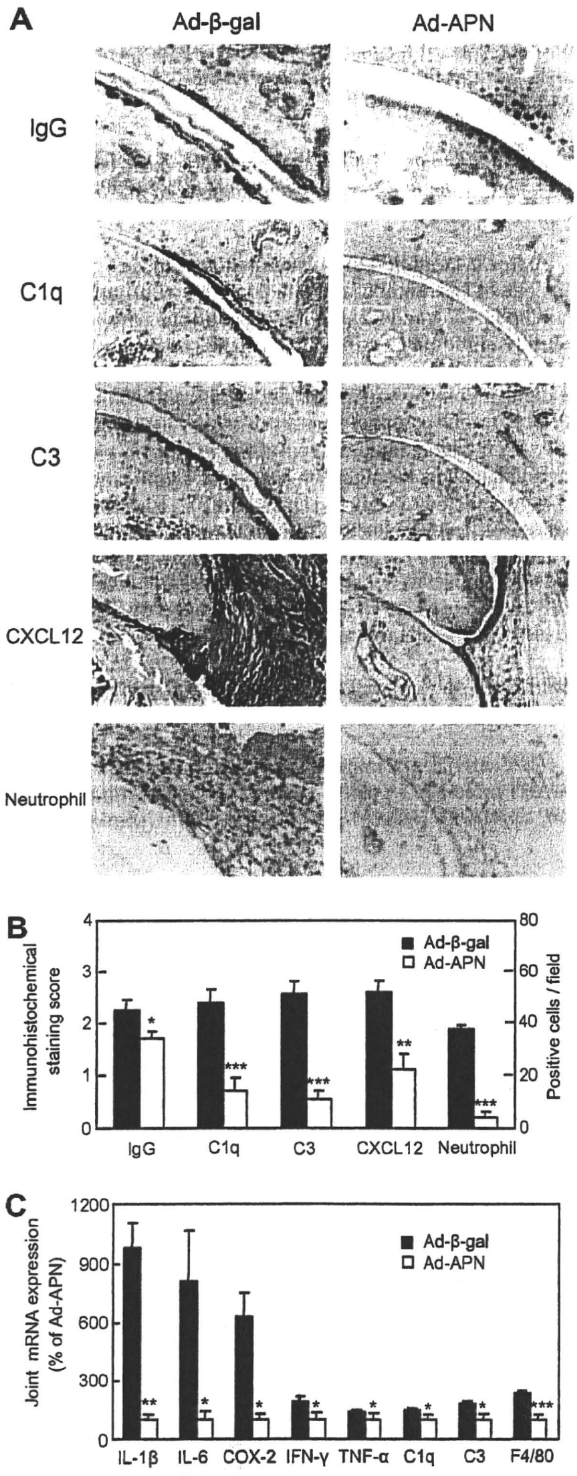

Fig. 3. Ad-APN inhibits complement deposition/expression and pro-inflammatory cytokine/enzyme expression in CIA mice. (A) Representative sections immunostained for IgG, C1q, C3, CXCL12, and neutrophil on the cartilage surface and synovium of the ankle joints of adenovirus-infected CIA mice (original magnification 200×). (B) Scoring of immunostained joint sections from adenovirus-infected CIA mice ($n = 16$ joints in each group). (C) mRNA expression levels in forepaws of adenovirus-infected CIA mice. ($n = 6$ joints in each group). Values are normalized to the level of 36B4 mRNA. $^{*}P < 0.05$, $^{**}P < 0.01$, $^{***}P < 0.001$, versus Ad-β-gal-infected CIA mice.

mice produced less IL-1β in all conditions, and less TNF-α in response to LPS *in vitro* (Fig. 4B). Finally, analysis of bone erosion of the distal tibia using μCT revealed that trabecular bone volume were significantly decreased in Ad-β-gal-infected CIA mice compared to those in Ad-APN-infected CIA mice (Fig. 4C). In addition, the number of TRAP-positive cells was significantly decreased in ankle joints of Ad-APN-infected CIA mice (Fig. 4D).

Discussion

In the present study, we demonstrated for the first time that Ad-APN significantly improved joint inflammation and bone erosion in CIA mice. There were no significant differences in anti-CII IgG, C1q, and C3 levels between Ad-APN and Ad-β-gal infected CIA mice (Fig. 2E and F), indicating that Ad-APN has little effect on humoral immunity. On the other hand, C1q and C3 deposition were markedly suppressed on the cartilage surface of Ad-APN-infected CIA mice (Fig. 3A and B). Therefore, we investigated the direct effect of APN on complement activation. APN has a substantial sequence similarity to C1q, and also binds to C1q receptor [15]. In addition, we confirmed the binding between human recombinant APN from mammalian cells and human C1q *in vitro* as reported previously [16]. However, in our preliminary experiments, this recombinant APN did not alter C1q binding to adherent CII-IC [11], CII-IC-induced mouse serum C3 activation (mainly involves classical pathway) [11], or zymosan-induced mouse serum C3 activation (mainly involves alternative pathway) [10] *in vitro* (data not shown). To elucidate the direct effect of APN on the complement activation, further *in vivo* and *in vitro* analyses are required.

We showed marked suppression of C1q and C3 deposition, accompanied by significant downregulation of C1q, C3, and F4/80 mRNAs in the Ad-APN-infected CIA joints (Fig. 3). A previous report demonstrated that APN inhibited the expression of endothelial adhesion molecules induced by TNF-α, and consequent transendothelial migration of monocytes [17]. In addition, TNF-α-induced vascular permeability is required for the migration of inflammatory cells into the joint and development of inflammatory process in mouse arthritis models [1], and APN was reported to inhibit TNF-α-induced hyperpermeability in endothelial cells [18]. Our group demonstrated that APN was protective against murine colitis through inhibition of macrophages infiltration and release of pro-inflammatory cytokines [19]. Considering that C1q is mainly produced by monocyte/macrophage linage [20], and C3 is produced by liver and inflamed synoviocytes [21], reduced accumulation of F4/80 positive cells and consequent C3 production by inflamed synovium should result in suppression of complement deposition and pro-inflammatory cytokine production in the CIA joints.

We also observed that Ad-APN suppressed synovial deposition of CXCL12. CXCL12 is a chemokine anchored to heparan sulfate (HS) proteoglycans on endothelial cells of RA synovium [22], and acts as a critical chemoattractant in the pathogenesis of CIA [23]. APN inhibits the binding of CXCL12 to HS, and alters the distribution of CXCL12 at the site of inflammation [24]. Taken together, Ad-APN may improve joint inflammation through decreased CXCL12 deposition in CIA synovium.

Previous studies showed that the cellular immunity, represented by the activity of immunocytes of lymph nodes or spleen, is causally associated with the disease activity in CIA mice [25]. In this study, Ad-APN marginally reduced DLN cells proliferation (Fig. 4A), and significantly suppressed IL-1β production and TNF-α production from splenocytes (Fig. 4B). These results indicate that Ad-APN could suppress disease activity of CIA partially through inhibition of cellular immunity.

In this study, Ad-APN reduced the number of TRAP-positive cells and resulted in amelioration of bone erosion in the joints of CIA mice (Fig. 4C and D). Previously, we and others reported that

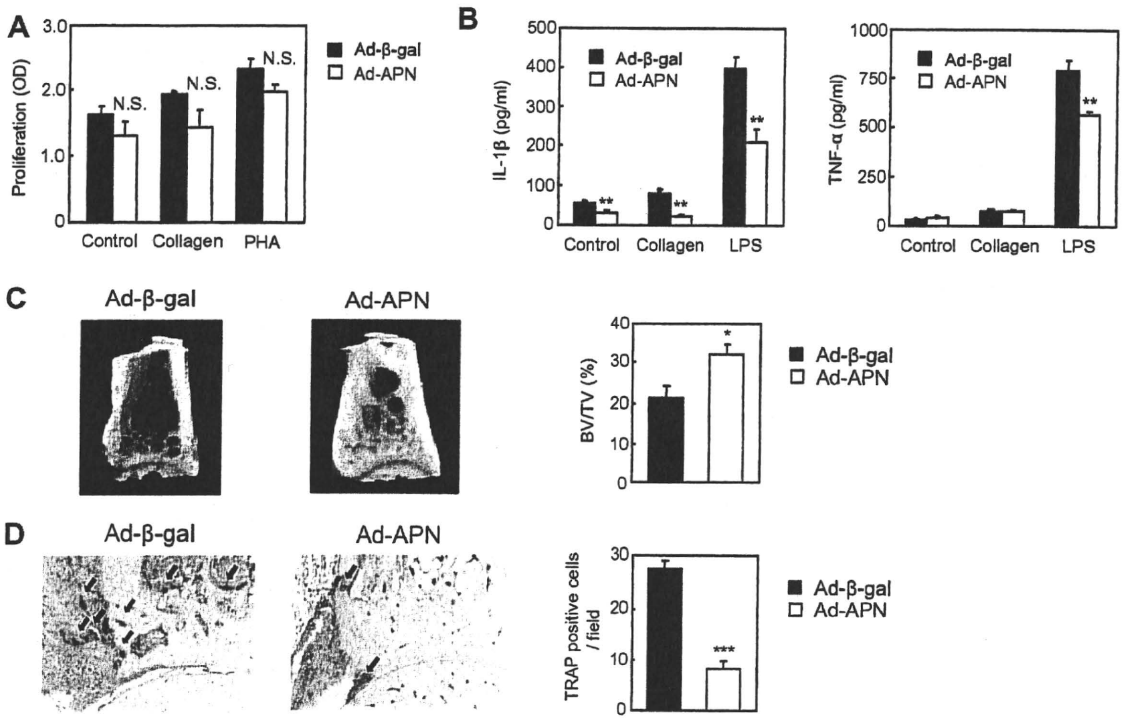

Fig. 4. Effects of Ad-APN on DLN cell proliferation and pro-inflammatory cytokine production from splenocytes, and bone erosion in CIA. All samples were obtained on day 35. (A) Proliferative response of DLN cells obtained from adenovirus-infected CIA mice. Isolated cells from lymph nodes were cultured for 72 h without (control) or with either 50 μg/ml heat-denatured chicken CII or 5 μg/ml phytohemagglutinin (PHA). (B) Production of pro-inflammatory cytokine by splenocytes from adenovirus-infected CIA mice. IL-1β and TNF-α levels were measured in supernatants of splenocytes by specific ELISA. (C) Three-dimensional μCT scan of the distal tibia of adenovirus-infected CIA mice. Trabecular bone volume is expressed as percentage of total tissue volume (BV/TV [%]) ($n = 4$ joints in each group). (D) Reduced number of osteoclasts in Ad-APN-infected CIA mice joints. Sections of ankle joints stained with TRAP (original magnification 100×). The number of TRAP-positive cells was counted in 5 randomly selected fields ($n = 8$ joints in each group). NS = not significant, $^{*}P < 0.05$, $^{**}P < 0.01$, $^{***}P < 0.001$, versus Ad-β-gal-infected CIA mice.

APN inhibits osteoclasts differentiation in RAW264 cells [26] and mouse bone marrow macrophages [9]. Collectively, besides anti-inflammatory effects in the joints, Ad-APN might directly inhibits bone erosion of CIA mice by inhibiting osteoclasts differentiation.

The present study demonstrates for the first time that systemic APN delivery provides protection against the development of inflammatory arthritis in a murine model, through several anti-inflammatory mechanisms. The results provide new insights on the role of APN in inflammatory arthritis and new strategies for the treatment.

Acknowledgments

We are grateful to Dr. T. Maeda for great help with the experiments. We also thank M. Shinkawa and F. Katsube for the excellent support in tissue processing for histological analysis. This work was supported by grants from the Ministry of Health, Labour, and Welfare of Japan.

Appendix A. Supplementary data

Supplementary data associated with this article can be found, in the online version, at doi:10.1016/j.bbrc.2008.11.005.

References

[1] J.A. Luross, N.A. Williams, The genetic and immunopathological processes underlying collagen-induced arthritis, Immunology 103 (2001) 407–416.
[2] P.E. Scherer, S. Williams, M. Fogliano, G. Baldini, H.F. Lodish, A novel serum protein similar to C1q, produced exclusively in adipocytes, J. Biol. Chem. 270 (1995) 26746–26749.
[3] M.C. Wulster-Radcliffe, K.M. Ajuwon, J. Wang, J.A. Christian, M.E. Spurlock, Adiponectin differentially regulates cytokines in porcine macrophages, Biochem. Biophys. Res. Commun. 316 (2004) 924–929.
[4] L. Senolt, K. Pavelka, D. Housa, M. Haluzik, Increased adiponectin is negatively linked to the local inflammatory process in patients with rheumatoid arthritis, Cytokine 35 (2006) 247–252.
[5] C.H. Tang, Y.C. Chiu, T.W. Tan, R.S. Yang, W.M. Fu, Adiponectin enhances IL-6 production in human synovial fibroblast via an AdipoR1 receptor, AMPK, p38, and NF-kappa B pathway, J. Immunol. 179 (2007) 5483–5492.
[6] N. Maeda, M. Takahashi, T. Funahashi, S. Kihara, H. Nishizawa, K. Kishida, H. Nagaretani, M. Matsuda, R. Komuro, N. Ouchi, H. Kuriyama, K. Hotta, T. Nakamura, I. Shimomura, Y. Matsuzawa, PPARgamma ligands increase expression and plasma concentrations of adiponectin, an adipose-derived protein, Diabetes 50 (2001) 2094–2099.
[7] S. Nakae, A. Nambu, K. Sudo, Y. Iwakura, Suppression of immune induction of collagen-induced arthritis in IL-17-deficient mice, J. Immunol. 171 (2003) 6173–6177.
[8] E. Gonzalez-Rey, A. Chorny, N. Varela, F. O'Valle, M. Delgado, Therapeutic effect of urocortin on collagen-induced arthritis by down-regulation of inflammatory and Th1 responses and induction of regulatory T cells, Arthritis Rheum. 56 (2007) 531–543.
[9] K. Oshima, A. Nampei, M. Matsuda, M. Iwaki, A. Fukuhara, J. Hashimoto, H. Yoshikawa, I. Shimomura, Adiponectin increases bone mass by suppressing osteoclast and activating osteoblast, Biochem. Biophys. Res. Commun. 331 (2005) 520–526.
[10] N.K. Banda, D. Kraus, A. Vondracek, L.H. Huynh, A. Bendele, V.M. Holers, W.P. Arend, Mechanisms of effects of complement inhibition in murine collagen-induced arthritis, Arthritis Rheum. 46 (2002) 3065–3075.
[11] N.K. Banda, K. Takahashi, A.K. Wood, V.M. Holers, W.P. Arend, Pathogenic complement activation in collagen antibody-induced arthritis in mice requires amplification by the alternative pathway, J. Immunol. 179 (2007) 4101–4109.
[12] A. Bendele, T. McAbee, G. Sennello, J. Frazier, E. Chlipala, D. McCabe, Efficacy of sustained blood levels of interleukin-1 receptor antagonist in animal models of arthritis: comparison of efficacy in animal models with human clinical data, Arthritis Rheum. 42 (1999) 498–506.
[13] N.K. Banda, J.M. Thurman, D. Kraus, A. Wood, M.C. Carroll, W.P. Arend, V.M. Holers, Alternative complement pathway activation is essential for inflammation and joint destruction in the passive transfer model of collagen-induced arthritis, J. Immunol. 177 (2006) 1904–1912.

[14] Z. Liu, X. Xu, H.C. Hsu, A. Tousson, P.A. Yang, Q. Wu, C. Liu, S. Yu, H.G. Zhang, J.D. Mountz, CII-DC-AdTRAIL cell gene therapy inhibits infiltration of CII-reactive T cells and CII-induced arthritis, J. Clin. Invest. 112 (2003) 1332–1341.
[15] T. Yokota, K. Oritani, I. Takahashi, J. Ishikawa, A. Matsuyama, N. Ouchi, S. Kihara, T. Funahashi, A.J. Tenner, Y. Tomiyama, Y. Matsuzawa, Adiponectin, a new member of the family of soluble defense collagens, negatively regulates the growth of myelomonocytic progenitors and the functions of macrophages, Blood 96 (2000) 1723–1732.
[16] P.W. Peake, Y. Shen, A. Walther, J.A. Charlesworth, Adiponectin binds C1q and activates the classical pathway of complement, Biochem. Biophys. Res. Commun. 367 (2008) 560–565.
[17] N. Ouchi, S. Kihara, Y. Arita, K. Maeda, H. Kuriyama, Y. Okamoto, K. Hotta, M. Nishida, M. Takahashi, T. Nakamura, S. Yamashita, T. Funahashi, Y. Matsuzawa, Novel modulator for endothelial adhesion molecules: adipocyte-derived plasma protein adiponectin, Circulation 100 (1999) 2473–2476.
[18] S.Q. Xu, K. Mahadev, X. Wu, L. Fuchsel, S. Donnelly, R.G. Scalia, B.J. Goldstein, Adiponectin protects against angiotensin ii or tumor necrosis factor {alpha}-induced endothelial cell monolayer hyperpermeability. Role of cAMP/PKA signaling, Arterioscler Thromb. Vasc. Biol. (2008).
[19] T. Nishihara, M. Matsuda, H. Araki, K. Oshima, S. Kihara, T. Funahashi, I. Shimomura, Effect of adiponectin on murine colitis induced by dextran sulfate sodium, Gastroenterology 131 (2006) 853–861.
[20] Y. Takemura, N. Ouchi, R. Shibata, T. Aprahamian, M.T. Kirber, R.S. Summer, S. Kihara, K. Walsh, Adiponectin modulates inflammatory reactions via calreticulin receptor-dependent clearance of early apoptotic bodies, J. Clin. Invest. 117 (2007) 375–386.
[21] P.A. Monach, A. Verschoor, J.P. Jacobs, M.C. Carroll, A.J. Wagers, C. Benoist, D. Mathis, Circulating C3 is necessary and sufficient for induction of autoantibody-mediated arthritis in a mouse model, Arthritis Rheum. 56 (2007) 2968–2974.
[22] J.L. Pablos, B. Santiago, M. Galindo, C. Torres, M.T. Brehmer, F.J. Blanco, F.J. Garcia-Lazaro, Synoviocyte-derived CXCL12 is displayed on endothelium and induces angiogenesis in rheumatoid arthritis, J. Immunol. 170 (2003) 2147–2152.
[23] B. De Klerck, L. Geboes, S. Hatse, H. Kelchtermans, Y. Meyvis, K. Vermeire, G. Bridger, A. Billiau, D. Schols, P. Matthys, Pro-inflammatory properties of stromal cell-derived factor-1 (CXCL12) in collagen-induced arthritis, Arthritis Res. Ther. 7 (2005) R1208–1220.
[24] H. Masaie, K. Oritani, T. Yokota, I. Takahashi, T. Shirogane, H. Ujiie, M. Ichii, N. Saitoh, T. Maeda, R. Tanigawa, K. Oka, Y. Hoshida, Y. Tomiyama, Y. Kanakura, Adiponectin binds to chemokines via the globular head and modulates interactions between chemokines and heparan sulfates, Exp. Hematol. 35 (2007) 947–956.
[25] N.K. Banda, A. Vondracek, D. Kraus, C.A. Dinarello, S.H. Kim, A. Bendele, G. Senaldi, W.P. Arend, Mechanisms of inhibition of collagen-induced arthritis by murine IL-18 binding protein, J. Immunol. 170 (2003) 2100–2105.
[26] N. Yamaguchi, T. Kukita, Y.J. Li, N. Kamio, S. Fukumoto, K. Nonaka, Y. Ninomiya, S. Hanazawa, Y. Yamashita, Adiponectin inhibits induction of TNF-alpha/RANKL-stimulated NFATc1 via the AMPK signaling, FEBS Lett. 582 (2008) 451–456.

Clin Rheumatol (2009) 28:445–451
DOI 10.1007/s10067-008-1074-y

ORIGINAL ARTICLE

Serum adiponectin concentrations correlate with severity of rheumatoid arthritis evaluated by extent of joint destruction

Kosuke Ebina · Atsunori Fukuhara · Wataru Ando · Makoto Hirao · Tadashi Koga · Kazuya Oshima · Morihiro Matsuda · Kazuhisa Maeda · Tadashi Nakamura · Takahiro Ochi · Iichiro Shimomura · Hideki Yoshikawa · Jun Hashimoto

Received: 12 October 2008 /Revised: 30 November 2008 /Accepted: 3 December 2008 /Published online: 16 December 2008

Abstract Adiponectin is a hormone released by adipose tissue with antidiabetic, antiatherogenic, and anti-inflammatory properties. The present observational study focused on the relation between serum adiponectin level and the disease severity of established rheumatoid arthritis (RA). Ninety patients with more than 5-year diagnosis of RA and 42 age- and BMI-matched control were enrolled. The severity of RA was evaluated according to the number of destructed joints of overall 68 joints on plain radiographs (37 patients had mild RA and 53 had severe RA). Serum adiponectin level was significantly higher in the severe RA group (17.7±6.7 μg/ml) than in the control (9.1±3.8 μg/ml) and mild RA groups (13.9±6.5 μg/ml) (control vs. mild RA group, $P<0.001$; mild RA vs. severe RA group, $P<0.01$). These results suggest that increased number of joint destruction is associated with hyperadiponectinemia in established RA patients.

Keywords Adiponectin · Disease severity · Number of joint destruction · Rheumatoid arthritis

Introduction

Adiponectin is a hormone released by adipose tissue and has various biological properties, such as antidiabetic [1], antiatherogenic [2], and anti-inflammatory effects [3]. Part

K. Ebina · W. Ando · M. Hirao · K. Oshima · H. Yoshikawa · J. Hashimoto (✉)
Department of Orthopaedics, Graduate School of Medicine,
Osaka University,
2-2 Yamadaoka,
Suita, Osaka 565-0871, Japan
e-mail: junha@ort.med.osaka-u.ac.jp

K. Ebina · A. Fukuhara · M. Matsuda · K. Maeda · T. Nakamura · I. Shimomura
Department of Metabolic Medicine, Graduate School of Medicine,
Osaka University,
2-2 Yamadaoka,
Suita, Osaka 565-0871, Japan

T. Koga
Biometrics Department,
Shin Nippon Biomedical Laboratories, Ltd,
2438 Miyanoura,
Kagoshima, Kagoshima 891-1394, Japan

M. Matsuda
Division of Analysis for Pathophysiology,
Institute of Clinical Research,
National Hospital Organization Kure Medical Center,
Kure, Hiroshima 737-0023, Japan

M. Matsuda
Department of Internal Medicine,
National Hospital Organization Kure Medical Center,
Kure, Hiroshima 737-0023, Japan

T. Ochi
Osaka Police Hospital,
10-31 Kitayama-cho, Tennoji-ku,
Osaka 543-0035, Japan

of these effects is mediated by suppressing the production of tumor necrosis factor (TNF)-α and interleukin (IL)-6 by activated macrophage [3]. In addition, it has been reported that adiponectin stimulates the proliferation and differentiation of human osteoblasts [4] and suppresses the differentiation of osteoclasts [5], suggesting that adiponectin may play a role in rheumatoid arthritis (RA).

A recent clinical study showed that serum adiponectin concentrations are higher in RA patients than in healthy control [6, 7]. In addition, adiponectin induces the production of pro-inflammatory IL-6 from RA synovial fibroblasts in vitro [8], suggesting that adiponectin is a potent driving force of arthritis. On the other hand, another report demonstrated that adiponectin concentrations correlated negatively with the number of leukocytes in the synovial fluid of RA patients [7], indicating that adiponectin is a counterpart of the local inflammatory process. Thus, the role of adiponectin in RA is controversial. In a step to define the role of adiponectin in RA, the present study was designed to investigate the correlation between serum adiponectin level and RA disease severity.

Materials and methods

Patients

We have previously reported that serum adiponectin level is significantly higher in females than in males and negatively correlates with body mass index (BMI) [9]. In addition, previous reports have demonstrated that most of the progression of joint damage in RA occurs during the first years of the disease and decreases thereafter [10, 11]. Therefore, to investigate the correlation between serum adiponectin level and disease severity and joint destruction in established RA, 90 female patients with more than 5-year history of RA were enrolled in this study. RA was diagnosed based on the 1987 revised American College of Rheumatology (ACR) criteria [12]. The first assessment was carried out from September to November, 2005, and 18 patients were enrolled in the second assessment from March to April, 2008, about 2.5 years after the first assessment. Sixty-five patients (72.2%) were treated with oral prednisolone and 48 patients (53.3%) with methotrexate. All patients were followed-up at Osaka University Hospital.

For non-RA controls, 42 age- and BMI-matched women who underwent health examination at the institutions that participated in the Japanese Visceral Fat Syndrome (J-VFS) Study Committee of the Ministry of Health and Welfare of Japan and subjects who visited Osaka University Hospital for health check were enrolled in the present study [13]. Patients treated with antihypertensive, antidiabetic, or antihyperlipidemic regimen or patients who met the definition of each disease indicated in the relevant guidelines were defined as having hypertension, diabetes, and hyperlipidemia, respectively. Patients treated with drugs influencing serum adiponectin levels, such as anti-TNF-α [14, 15], insulin [16], thiazolidinediones [17], telmisartan [18], glimepiride [19], and all other biologics were excluded in this study. The study was approved by the Ethical Committee of Osaka University School of Medicine and written informed consent was obtained from each patient.

Assessment of disease severity and disease activity

The severity of RA was evaluated by the number of joints with erosions among 68 joints of whole body using plain radiographs, as described previously [20]. Joint erosion was defined as changes equal to or more severe than stage II according to the criteria of Steinbocker et al. [21]. Patients were classified according to disease severity as described previously [22]. Briefly, the least erosive subset (LES) group exhibited erosions in less than 20 joints and erosive articular changes limited to the small peripheral joints of hands or feet. The more erosive subset (MES) group had erosions in more than 21 joints and erosive articular changes in large axial joints. The most erosive subset with mutilating disease (MUD) group, that had erosions in more than 46 joints, and almost all joints were extensively damaged in the early period of RA. In this study, we categorized LES patients as the "mild RA group" (n=37), and MES/MUD patients as the "severe RA group" (n=53). Disease activity score including a 28 joint count/CRP (DAS28-CRP) was evaluated as described previously [23].

Measurement of serum adiponectin concentrations

Total serum adiponectin level (including all isoforms) was measured with an enzyme-linked immunosorbent assay (ELISA) kit (Otsuka Pharmaceutical, Tokyo, Japan), as reported previously [13].

Statistical analysis

Data are expressed as mean ± standard deviation (SD). Differences in variables between the mild and severe RA groups were assessed by the Mann–Whitney U test and the chi-square test. Changes in serum adiponectin levels between the first and second assessment was examined by the Wilcoxon's signed rank test. The influence of serum adiponectin level on other variables was investigated by calculating Spearman's correlation coefficients. The correlation between BMI and disease severity was investigated by logistic regression analysis. Conditional multivariate logistic regression models were constructed and odds ratios (ORs) and 95% confidence intervals (95% CI) were cal-

culated to investigate the association of serum adiponectin level on disease severity, with adjustment for BMI. To investigate the cutoff value for serum adiponectin, a value yielding 80% correspondence to the severity of RA was estimated by a logistic regression model and statistical significance was estimated by Fisher's exact test. Probability values of less than 0.05 were considered statistically significant. All statistical analyses were carried out with SAS software version 9.1.3 (SAS Institute, Cary, NC, USA).

Results

Clinical and biochemical characteristics of the study subjects

There were no significant differences between mild and severe RA groups in age (60.8±11.0 vs. 61.7±11.7 years), disease duration (15.5±6.9 vs. 17.3±6.8 years), body mass index (22.1±3.4 vs. 20.8±3.0 kg/m^2), and prevalence of hypertension (18.8% vs. 28.3%), diabetes (16.2 vs. 18.9%), and hyperlipidemia (21.6 vs. 24.5%). The age and BMI of subjects of the control group were 61.0±11.4 years and 21.9±3.2 kg/m^2, respectively. The prevalence of each

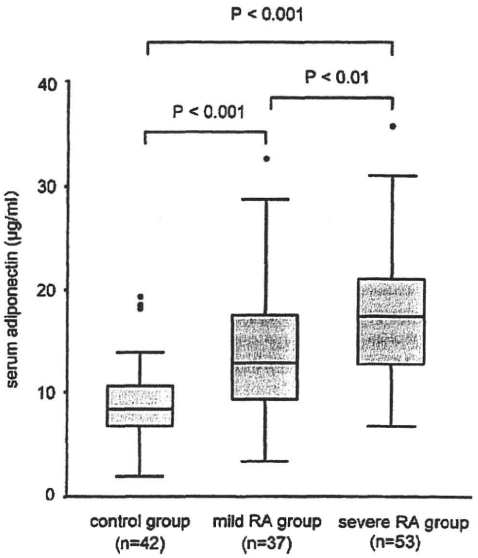

Fig. 1 Box-and-whisker plots of serum adiponectin levels in the control group, mild RA group, and severe RA group evaluated by the number of joint destruction in 68 joints on plain radiograph. The mean serum level of adiponectin was significantly higher in the severe RA group (17.7±6.7 μg/ml) than in the control (9.1±3.8 μg/ml) or mild RA group (13.9±6.5 μg/ml) (control vs. mild RA group: $P<0.001$, mild RA vs. severe RA group: $P<0.01$, control vs. severe RA group: $P<0.001$)

Table 1 Baseline demographic, laboratory, and clinical characteristics of the two RA groups

	mild RA group (n=37)	severe RA group (n=53)	P[a] value
Age, years	60.8±11.0	61.7±11.7	NS
Duration of disease, years	15.5±6.9	17.3±6.8	NS
Body mass index, kg/m^2	22.1±3.4	20.8±3.0	NS
CRP, mg/l	0.9±1.3	1.9±2.0	0.003
MMP-3, ng/ml	146.5±150.9	222.8±177.6	0.047
IL-6, ρg/ml	14.5±36.0	18.1±26.2	NS
RF titer, IU/ml	158.1±417.0	235.7±366.9	NS
RF positivity, % patients	77.1%	82.7%	NS[b]
BAP, U/l	24.0±13.5	23.9±9.5	NS
iOC, ng/ml	6.9±3.5	6.7±7.3	NS
1CTP, ng/ml	4.9±1.9	6.5±3.1	0.010
uDPD, nmol/mmol creatinine	6.6±2.2	7.9±3.2	NS
DAS28-CRP	2.2±1.0	3.1±1.5	0.001
Prednisolone dosage, mg/day	2.2±2.5	4.3±3.6	0.001
Methotrexate dosage, mg/week	4.3±3.2	4.4±3.6	NS
Adiponectin, μg/ml	13.9±6.5	17.7±6.7	0.008

Data are mean ± SD

RA rheumatoid arthritis, *NS* not significant, *CRP* C-reactive protein, *MMP-3* matrix metalloproteinase-3, *IL-6* interleukin-6, *RF* rheumatoid factor, *BAP* bone-specific alkaline phosphatase, *iOC* intact osteocalcin, *1CTP* pyridinoline cross-linked carboxyterminal telopeptide of type 1 collagen, *uDPD* urinary deoxypyridinoline, *DAS28-CRP* disease activity score including a 28-joint count/CRP

[a] Except where otherwise indicated, determined by Mann–Whitney *U* test

[b] Except where otherwise indicated, determined by chi-square test

Table 2 Spearman's correlation analysis of the relation between serum adiponectin and other variables in all RA patients

Variable	r value	P value
Age, years	0.046	NS
Duration of disease, years	0.068	NS
Body mass index, kg/m^2	−0.269	0.011
CRP, mg/liter	0.078	NS
MMP-3, ng/ml	0.098	NS
IL-6, ρg/ml	0.120	NS
RF titer, IU/ml	−0.033	NS
BAP, U/l	−0.193	NS
iOC, ng/ml	−0.075	NS
1CTP, ng/ml	0.033	NS
uDPD, nmol/mmol creatinine	−0.002	NS
DAS28-CRP	0.096	NS
Prednisolone dosage, mg/day	0.040	NS

r value Spearman's rank correlation coefficient, *NS* not significant, *CRP* C-reactive protein, *MMP-3* matrix metalloproteinase-3, *IL-6* interleukin-6, *RF* rheumatoid factor, *BAP* bone-specific alkaline phosphatase, *iOC* intact osteocalcin, *1CTP* pyridinoline cross-linked carboxyterminal telopeptide of type 1 collagen, *uDPD* urinary deoxypyridinoline, *DAS28-CRP* disease activity score including a 28-joint count/CRP

Table 3 Results of Spearman's rank correlation analysis of the relation between adiponectin and other variables with a significant difference between the severe and mild RA groups

	CRP	MMP-3	1CTP	DAS28-CRP	Prednisolone	Adiponectin
CRP		0.574***	0.486***	0.717***	0.335**	0.078
MMP-3			0.331**	0.532***	0.510***	0.098
1CTP				0.389***	0.220*	0.033
DAS28-CRP					0.372**	0.096
Prednisolone						0.040

CRP C-reactive protein, *MMP-3* matrix metalloproteinase-3, *1CTP* pyridinoline cross-linked carboxyterminal telopeptide of type 1 collagen, *DAS28-CRP* disease activity score including a 28-joint count/CRP
*$P<0.05$; **$P<0.01$; ***$P<0.001$

disease in the control group was 0% for hypertension, 2.3% for diabetes, and 9.5% for hyperlipidemia. Patients of the severe RA group had a significantly higher serum C-reactive protein (CRP) ($P=0.003$), matrix metalloproteinase (MMP)-3 ($P=0.047$), pyridinoline cross-linked carboxyterminal telopeptide of type 1 collagen (1CTP) ($P=0.010$), disease activity score including a 28-joint count/CRP (DAS28-CRP) ($P=0.001$), and prednisolone dose ($P=0.001$) than the mild RA group (Table 1), reflecting high inflammatory state and bone resorption level in this group as described previously [24]. The mean serum level of adiponectin was significantly higher in the total RA group (16.1±6.8 μg/ml) than in the control group (9.1±3.8 μg/ml) ($P<0.001$). Moreover, the mean serum level of adiponectin was significantly higher in the severe RA group (17.7±6.7 μg/ml) than in the control (9.1±3.8 μg/ml) or mild RA group (13.9±6.5 μg/ml) (control vs. mild RA group, $P<0.001$; mild RA vs. severe RA group, $P<0.01$, control vs. severe RA group, $P<0.001$) (Fig. 1). Univariate analysis of the relationship between serum adiponectin level and other variables showed that adiponectin correlated negatively with BMI ($r=-0.269$, $P=0.011$), but did not correlate with other variables such as inflammatory markers, bone metabolism markers, DAS28-CRP, or the dose of prednisolone (Table 2). Calculation of Spearman's rank correlation coefficients for the variables with a significant difference between the mild and severe RA groups showed that CRP correlated with MMP-3 ($r=0.574$, $P<0.001$), 1CTP ($r=0.486$, $P<0.001$), DAS28-CRP($r=0.717$, $P<0.001$), and dose of prednisolone ($r=0.335$, $P<0.01$), while there was no significant correlation with adiponectin ($r=0.078$, $P>0.05$) (Table 3). In addition, the dose of prednisolone correlated with CRP, MMP-3, 1CTP, and DAS28-CRP, but not with adiponectin ($r=0.040$, $P>0.05$) (Table 3). Multivariate logistic regression analyses revealed that even when the odds ratios were adjusted for BMI, serum adiponectin level significantly correlates with disease severity of RA ($P=0.031$) (Table 4).

Cutoff point of serum adiponectin for severe RA

Figure 2 shows the histogram of serum adiponectin levels of patients of the mild and severe RA groups. For clinical translation, the cutoff levels were selected. The cutoff value for serum adiponectin level was estimated at 18 μg/ml, yielding 80% correspondence with the severity of RA. Among the patients with serum adiponectin level of ≥18 μg/ml, 81.3% (26/32) belonged to the severe RA group and 18.8% (6/32) belonged to the mild RA group. This cutoff line showed significant correlation with disease severity ($P<0.01$). The specificity of this cutoff value was 53.4% (31/58) (Table 5).

Changes in serum adiponectin levels and severity of RA during follow-up

To further investigate the time-course changes of serum adiponectin levels and severity of RA, 18 patients underwent a second assessment 2.5 years later (Fig. 3). The mean serum adiponectin level of all patients did not change significantly, although it showed tendency to increase (14.0±5.5 to 15.2±5.2 μg/ml; $P=0.07$). Furthermore, the mean serum adiponectin level did not change significantly within the RA group (10.8±5.8 to 12.4±5.8 μg/ml in the mild RA group, $P=0.122$ and 17.2±2.7 to 18.0±2.4 μg/ml in the severe RA group, $P=0.372$). Assessment of RA severity revealed that none of the mild RA patients progressed to severe RA (data not shown).

Table 4 Adjusted ORs of serum adiponectin level and BMI for disease severity of RA

	Adjusted OR	95% CI	*P* value
Adiponectin, μg/ml	1.085	1.007–1.168	0.031
BMI, kg/m^2	0.907	0.785–1.048	NS

ORs odds ratios, *95% CI* 95% confidence interval, *NS* not significant

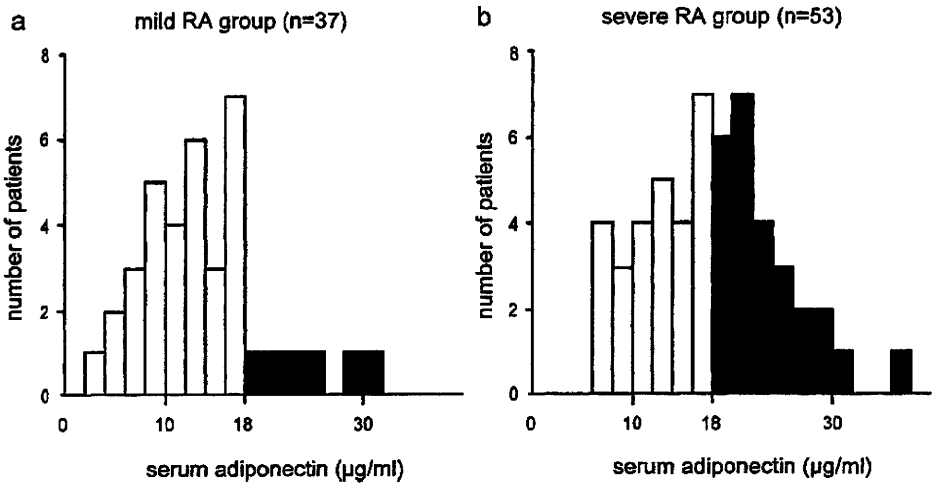

Fig. 2 Histograms showing the distribution of serum adiponectin levels in mild RA group (**a**) and severe RA group (**b**). Each column covers a serum adiponectin range of 2 μg/ml. When the cutoff value for adiponectin was set at 18 μg/ml, there was 80% correspondence with the severity of RA. Among patients with serum adiponectin levels ≥18 μg/ml, 81.3% (26/32) belonged to the severe RA group and 18.8% (6/32) belonged to the mild RA group

Discussion

The long-term functional prognosis of RA patients in daily life is mainly determined by the extent of damage in large joints such as the hip, knee, ankle, subtalar, shoulder, and elbow joints, rather than in small joints of the hands or feet. A previous report using Ochi's method demonstrated that MES and MUD groups underwent higher frequency of total knee or hip replacement than LES group (54.7% vs. 0.5%) [25], suggesting that Ochi's method offers some advantages for assessing large joint destruction [20, 25–27]. Therefore, we used Ochi's method to evaluate the severity of RA, to investigate the factors associated with the extent of overall joint destruction, especially in large joints [20]. Evaluation using this method revealed that markers associated with RA activity, such as CRP, MMP-3, 1CTP, and DAS28-CRP were all significantly higher in the severe RA group than in the mild RA group. These results were in agreement with previously published reports evaluated by the modified Sharp/van der Heijde method and Larsen's method (CRP [28], MMP-3 [29], 1CTP [30], and DAS [31]).

We showed for the first time that serum adiponectin levels were higher in the severe RA group than in control and mild RA groups. Interestingly, while other disease severity-related variables, such as MMP-3, 1CTP, DAS28-CRP, and dose of prednisolone correlated with CRP, serum adiponectin levels did not, in both the mild and severe RA groups (Table 3). It has been reported that serum TNF-α and CRP levels are elevated in RA patients [32, 33], and TNF-α, CRP, and corticosteroid markedly inhibit adiponectin gene expression in cultured adipocytes [16, 34]. Furthermore, anti-TNF-α therapy restored serum adiponectin level in RA patients [14, 15, 35]. On the other hand, despite elevated CRP levels and higher dose of treated oral prednisolone (corticosteroid), serum adiponectin levels were elevated in the severe RA group than in the mild

Table 5 Separation of mild and severe RA using a cutoff value for serum adiponectin of 18 μg/ml

	Serum adiponectin level	
	<18 μg/ml	≥18 μg/ml
Mild RA group (n)	31	6
Severe RA group (n)	27	26
% with severe RA	46.6%	81.3%

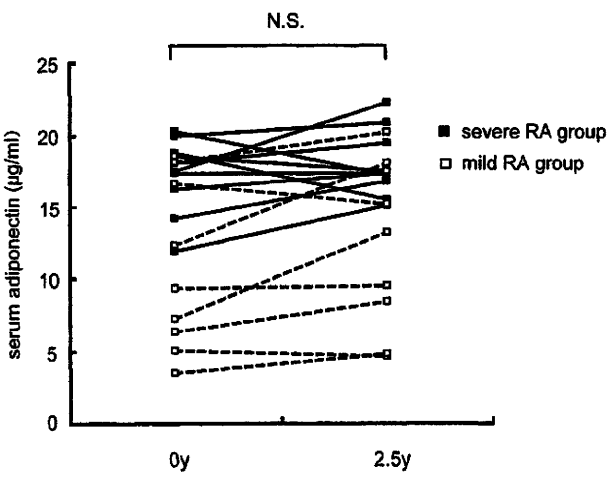

Fig. 3 Changes in serum adiponectin levels of 18 RA subjects in 2.5-year interval. The mean serum adiponectin level of the whole group was 14.0±5.5 μg/ml at baseline (0 years) and 15.2±5.2 μg/ml at follow-up (2.5 years, P=0.07); 10.8±5.8 vs. 12.4±5.8 μg/ml in mild RA group (P=0.122) and 17.2±2.7 vs. 18.0±2.4 μg/ml in severe RA group (P=0.372) and the change was not significant in either groups. None of the mild RA patients showed worsening to severe RA category during this period

RA group in the present study (Table 3). Considered together, serum adiponectin should be induced by unknown factors associated with the number of destructed joints, especially in large joints, and their effects should exceed the inhibitory effects of TNF-α, CRP, and prednisolone in RA patients. Recently, Fantuzzi [36] suggested that adiponectin promotes survival during periods of catabolism secondary to malnutrition and that hyperadiponectinemia may be the result of response to catabolic state in RA. Consequently, a catabolic state accompanied by joint destruction, especially in large joints, may be one of the strong inducer of serum adiponectin level.

It has been reported that a low BMI is a sensitive and independent predictor of radiographic progression of joint damage assessed by Larsen's method in RA [37, 38]. In this study, there was no significant difference in BMI between control, mild RA, and severe RA group (21.9±3.2 vs. 22.1± 3.4 vs. 20.8±3.0 kg/m^2). In addition, in total RA group, BMI showed only tendency of positive correlation with disease severity (P=0.059). However, under such condition, serum adiponectin levels were significantly higher in severe RA group than in the control and mild RA groups (Table 1, Fig. 1). Furthermore, multivariate logistic regression analyses revealed that even when the odds ratios were adjusted for BMI, serum adiponectin level significantly correlates with disease severity of RA (Table 4). Therefore, we speculate that serum adiponectin levels can be a better sensitive indicator of the expansion of joint destruction than BMI in RA patients. To further investigate the time course changes in serum adiponectin levels and severity of RA, 18 patients were assessed 2.5 years later. The results showed no significant change in serum adiponectin levels and none of the mild RA patients progressed to severe RA. The lack of change in the severity category during this period is compatible with previous reports indicating that most of the progression of joint damage in RA occurs during the first years of the disease and decrease thereafter [10, 11, 20]; and under such conditions, serum adiponectin level is relatively stable in established RA (disease duration ≥5 years).

For clinical translation of these findings, we determined the cutoff level of serum adiponectin level. The estimated cutoff levels estimated by the histogram of serum adiponectin level showed relatively high sensitivity (81.3%) but low specificity (53.4%) in this study (Fig. 2, Table 5), indicating that increased number of destructed joints may be one of the additive, but not a specific factor of high serum adiponectin level in RA. Consequently, prospective studies in early stage of RA (disease duration <5 years) and in large number of RA patients are needed to determine the cutoff level of adiponectin to be used as an indicator or predictor of destructed joints. In addition, to elucidate the effect of hyperadiponectinemia on the severity of RA, further animal experiments are needed.

Despite the limitation of observational study, we demonstrated that the severity of RA, evaluated by the number of destructed joints on plain radiographs detected in the whole skeleton, correlated with serum adiponectin concentrations. This finding should encourage further research to investigate the role of adiponectin in RA and design new adiponectin-based treatment strategies for RA.

Acknowledgments This work was supported by grants from the Ministry of Health, Labor, and Welfare of Japan.

Disclosures None.

References

1. Maeda N, Shimomura I, Kishida K, Nishizawa H, Matsuda M, Nagaretani H, Furuyama N, Kondo H, Takahashi M, Arita Y, Komuro R, Ouchi N, Kihara S, Tochino Y, Okutomi K, Horie M, Takeda S, Aoyama T, Funahashi T, Matsuzawa Y (2002) Diet-induced insulin resistance in mice lacking adiponectin/ACRP30. Nat Med 8:731–737
2. Matsuda M, Shimomura I, Sata M, Arita Y, Nishida M, Maeda N, Kumada M, Okamoto Y, Nagaretani H, Nishizawa H, Kishida K, Komuro R, Ouchi N, Kihara S, Nagai R, Funahashi T, Matsuzawa Y (2002) Role of adiponectin in preventing vascular stenosis. The missing link of adipo-vascular axis. J Biol Chem 277:37487–37491
3. Wulster-Radcliffe MC, Ajuwon KM, Wang J, Christian JA, Spurlock ME (2004) Adiponectin differentially regulates cytokines in porcine macrophages. Biochem Biophys Res Commun 316:924–929
4. Luo XH, Guo LJ, Yuan LQ, Xie H, Zhou HD, Wu XP, Liao EY (2005) Adiponectin stimulates human osteoblasts proliferation and differentiation via the MAPK signaling pathway. Exp Cell Res 309:99–109
5. Oshima K, Nampei A, Matsuda M, Iwaki M, Fukuhara A, Hashimoto J, Yoshikawa H, Shimomura I (2005) Adiponectin increases bone mass by suppressing osteoclast and activating osteoblast. Biochem Biophys Res Commun 331:520–526
6. Otero M, Lago R, Gomez R, Lago F, Dieguez C, Gomez-Reino JJ, Gualillo O (2006) Changes in plasma levels of fat-derived hormones adiponectin, leptin, resistin and visfatin in patients with rheumatoid arthritis. Ann Rheum Dis 65:1198–1201
7. Senolt L, Pavelka K, Housa D, Haluzik M (2006) Increased adiponectin is negatively linked to the local inflammatory process in patients with rheumatoid arthritis. Cytokine 35:247–252
8. Ehling A, Schaffler A, Herfarth H, Tarner IH, Anders S, Distler O, Paul G, Distler J, Gay S, Scholmerich J, Neumann E, Muller-Ladner U (2006) The potential of adiponectin in driving arthritis. J Immunol 176:4468–4478
9. Arita Y, Kihara S, Ouchi N, Takahashi M, Maeda K, Miyagawa J, Hotta K, Shimomura I, Nakamura T, Miyaoka K, Kuriyama H, Nishida M, Yamashita S, Okubo K, Matsubara K, Muraguchi M, Ohmoto Y, Funahashi T, Matsuzawa Y (1999) Paradoxical decrease of an adipose-specific protein, adiponectin, in obesity. Biochem Biophys Res Commun 257:79–83
10. Sharp JT, Wolfe F, Mitchell DM, Bloch DA (1991) The progression of erosion and joint space narrowing scores in rheumatoid arthritis during the first twenty-five years of disease. Arthritis Rheum 34:660–668

11. van der Heijde DM, van Leeuwen MA, van Riel PL, Koster AM, van 't Hof MA, van Rijswijk MH, van de Putte LB (1992) Biannual radiographic assessments of hands and feet in a three-year prospective followup of patients with early rheumatoid arthritis. Arthritis Rheum 35:26–34
12. Arnett FC, Edworthy SM, Bloch DA, McShane DJ, Fries JF, Cooper NS, Healey LA, Kaplan SR, Liang MH, Luthra HS et al (1988) The American Rheumatism Association 1987 revised criteria for the classification of rheumatoid arthritis. Arthritis Rheum 31:315–324
13. Ryo M, Nakamura T, Kihara S, Kumada M, Shibazaki S, Takahashi M, Nagai M, Matsuzawa Y, Funahashi T (2004) Adiponectin as a biomarker of the metabolic syndrome. Circ J 68:975–981
14. Komai N, Morita Y, Sakuta T, Kuwabara A, Kashihara N (2007) Anti-tumor necrosis factor therapy increases serum adiponectin levels with the improvement of endothelial dysfunction in patients with rheumatoid arthritis. Mod Rheumatol 17:385–390
15. Nishida K, Okada Y, Nawata M, Saito K, Tanaka Y (2008) Induction of hyperadiponectinemia following long-term treatment of patients with rheumatoid arthritis with infliximab (IFX), an anti-TNF-alpha antibody. Endocr J 55:213–216
16. Fasshauer M, Klein J, Neumann S, Eszlinger M, Paschke R (2002) Hormonal regulation of adiponectin gene expression in 3T3-L1 adipocytes. Biochem Biophys Res Commun 290:1084–1089
17. Maeda N, Takahashi M, Funahashi T, Kihara S, Nishizawa H, Kishida K, Nagaretani H, Matsuda M, Komuro R, Ouchi N, Kuriyama H, Hotta K, Nakamura T, Shimomura I, Matsuzawa Y (2001) PPARgamma ligands increase expression and plasma concentrations of adiponectin, an adipose-derived protein. Diabetes 50:2094–2099
18. Yamada S, Ano N, Toda K, Kitaoka A, Shiono K, Inoue G, Atsuda K, Irie J (2008) Telmisartan but not candesartan affects adiponectin expression in vivo and in vitro. Hypertens Res 31:601–606
19. Koshiba K, Nomura M, Nakaya Y, Ito S (2006) Efficacy of glimepiride on insulin resistance, adipocytokines, and atherosclerosis. J Med Invest 53:87–94
20. Ochi T, Yonemasu K, Iwase R, Sasaki T, Tsuyama K, Ono K (1984) Serum C1q levels as a prognostic guide to articular erosions in patients with rheumatoid arthritis. Arthritis Rheum 27:883–887
21. Steinbrocker O, Traeger CH, Batterman RC (1949) Therapeutic criteria in rheumatoid arthritis. J Am Med Assoc 140:659–662
22. Wakitani S, Murata N, Toda Y, Ogawa R, Kaneshige T, Nishimura Y, Ochi T (1997) The relationship between HLA-DRB1 alleles and disease subsets of rheumatoid arthritis in Japanese. Br J Rheumatol 36:630–636
23. Inoue E, Yamanaka H, Hara M, Tomatsu T, Kamatani N (2007) Comparison of Disease Activity Score (DAS)28- erythrocyte sedimentation rate and DAS28-C-reactive protein threshold values. Ann Rheum Dis 66:407–409
24. Toritsuka Y, Nakamura N, Lee SB, Hashimoto J, Yasui N, Shino K, Ochi T (1997) Osteoclastogenesis in iliac bone marrow of patients with rheumatoid arthritis. J Rheumatol 24:1690–1696
25. Wakitani S, Kuwata K, Imoto K, Murata N, Oonishi H, Ochi T (1998) Knee and/or hip joint destruction in rheumatoid arthritis is associated with HLA-DRB1*0405 in Japanese patients. Clin Rheumatol 17:485–488
26. Momohara S, Yamanaka H, Holledge MM, Mizumura T, Ikari K, Okada N, Kamatani N, Tomatsu T (2004) Cartilage oligomeric matrix protein in serum and synovial fluid of rheumatoid arthritis: potential use as a marker for joint cartilage damage. Mod Rheumatol 14:356–360
27. Shibuya K, Hagino H, Morio Y, Teshima R (2002) Cross-sectional and longitudinal study of osteoporosis in patients with rheumatoid arthritis. Clin Rheumatol 21:150–158
28. Jansen LM, van der Horst-Bruinsma IE, van Schaardenburg D, Bezemer PD, Dijkmans BA (2001) Predictors of radiographic joint damage in patients with early rheumatoid arthritis. Ann Rheum Dis 60:924–927
29. Young-Min S, Cawston T, Marshall N, Coady D, Christgau S, Saxne T, Robins S, Griffiths I (2007) Biomarkers predict radiographic progression in early rheumatoid arthritis and perform well compared with traditional markers. Arthritis Rheum 56:3236–3247
30. Aman S, Paimela L, Leirisalo-Repo M, Risteli J, Kautiainen H, Helve T, Hakala M (2000) Prediction of disease progression in early rheumatoid arthritis by ICTP, RF and CRP. A comparative 3-year follow-up study. Rheumatology (Oxford) 39:1009–1013
31. Welsing PM, van Gestel AM, Swinkels HL, Kiemeney LA, van Riel PL (2001) The relationship between disease activity, joint destruction, and functional capacity over the course of rheumatoid arthritis. Arthritis Rheum 44:2009–2017
32. Barrera P, Boerbooms AM, Janssen EM, Sauerwein RW, Gallati H, Mulder J, de Boo T, Demacker PN, van de Putte LB, van der Meer JW (1993) Circulating soluble tumor necrosis factor receptors, interleukin-2 receptors, tumor necrosis factor alpha, and interleukin-6 levels in rheumatoid arthritis. Longitudinal evaluation during methotrexate and azathioprine therapy. Arthritis Rheum 36:1070–1079
33. Cohick CB, Furst DE, Quagliata S, Corcoran KA, Steere KJ, Yager JG, Lindsley HB (1994) Analysis of elevated serum interleukin-6 levels in rheumatoid arthritis: correlation with erythrocyte sedimentation rate or C-reactive protein. J Lab Clin Med 123:721–727
34. Yuan G, Chen X, Ma Q, Qiao J, Li R, Li X, Li S, Tang J, Zhou L, Song H, Chen M (2007) C-reactive protein inhibits adiponectin gene expression and secretion in 3T3-L1 adipocytes. J Endocrinol 194:275–281
35. Serelis J, Kontogianni MD, Katsiougiannis S, Bletsa M, Tektonidou MG, Skopouli FN (2008) Effect of anti-TNF treatment on body composition and serum adiponectin levels of women with rheumatoid arthritis. Clin Rheumatol 27:795–797
36. Fantuzzi G (2008) Adiponectin and inflammation: consensus and controversy. J Allergy Clin Immunol 121:326–330
37. van der Helm-van Mil AH, van der Kooij SM, Allaart CF, Toes RE, Huizinga TW (2008) A high body mass index has a protective effect on the amount of joint destruction in small joints in early rheumatoid arthritis. Ann Rheum Dis 67:769–774
38. Westhoff G, Rau R, Zink A (2007) Radiographic joint damage in early rheumatoid arthritis is highly dependent on body mass index. Arthritis Rheum 56:3575–3582

J Shoulder Elbow Surg (2009) 18, 33-37

ELSEVIER

JOURNAL OF SHOULDER AND ELBOW SURGERY

www.elsevier.com/locate/ymse

Morphologic analysis of the medullary canal in rheumatoid elbows

Akira Goto, MD, PhD[a,*], Tsuyoshi Murase, MD, PhD[a], Jun Hashimoto, MD, PhD[a], Kunihiro Oka, MD, PhD[a], Hideki Yoshikawa, MD, PhD[a], Kazuomi Sugamoto, MD, PhD[b]

[a]*Department of Orthopaedic Surgery, Osaka University Graduate School of Medicine, Suita, Osaka, Japan*
[b]*Department of Orthopaedic Biomaterial Science, Osaka University Graduate School of Medicine, Suita, Osaka, Japan*

Summary Total elbow arthroplasty is a standard approach for patients with arthritic elbows. To design appropriate stems for elbow prostheses, it is important to understand the shape of the medullary canals. The purpose of this study was to evaluate the shape and size of the medullary canals from normal cadavers and rheumatoid arthritis patients. These canals were measured based on geometric constructions of the 3-dimensional bone models generated from computed tomography images. The cross-sectional area of the medullary canals in rheumatoid arthritis patients decreased near the elbow joint as a result of morphologic changes after a long-standing inflammatory reaction. When designing the press-fit component of the humerus, an increase in the width of the transverse diameter of the intramedullary stem could increase stability in the canal. In contrast, for the ulnar component, such morphologic changes would impose difficulty in placing the press-fit model despite an anatomically designed stem. Therefore, a cement technique would be required for improved stabilization of the ulnar component.

Rheumatoid arthritis (RA) is an inflammatory condition, typified by synovial proliferation, that can affect multiple joints, with elbow involvement being the most common in nearly half of RA cases.[12] Total elbow arthroplasty (TEA) in rheumatoid patients is now a widely accepted therapeutic alternative for advanced elbow destruction. The advantage of TEA over simple synovectomy is that it can reduce pain, improve the range of joint motion, and provide long-term pain relief. However, loosening of the implants is one of the major complications and a primary concern. Although the improvement in surgical technique and prosthetic design has led to increased success with TEA, high rates of humeral component loosening have been reported previously.[5,8,18,23,26] Stem design of the prosthesis is considered an important factor that influences loosening of the implant. Data on the geometry of the medullary canals of the distal humerus and proximal ulna should help to design stems for elbow prostheses, which could occupy the medullary cavity, increase its stability with regard to the bone, and decrease the rate of loosening. However, in these patients, it is difficult to evaluate the morphologic analysis appropriately, based only on plain radiographs. In addition, RA patients have shown a restricted range of motion of the elbow with occasional valgus deformity because of erosive changes. Therefore, with only an axial computed tomography (CT) scan, it is difficult to evaluate the morphology accurately. Recent advancements in computer technology have enabled us to determine the precise geometry of the medullary canals generated from the CT data. We have

*Reprint requests: Akira Goto, MD, PhD, Department of Orthopaedic Surgery, Osaka University Graduate School of Medicine, 2-2, Yamada-oka, Suita, Osaka 565-0871, Japan.
E-mail address: goto-akira@umin.ac.jp (A. Goto).

1058-2746/2009/$36.00 - see front matter © 2009 Journal of Shoulder and Elbow Surgery Board of Trustees.
doi:10.1016/j.jse.2008.07.002

constructed 3-dimensional (3D) bone models and resliced the medullary canal vertically along its longitudinal axis to obtain accurate measurements. The purpose of this study was to evaluate the geometry of the medullary canals of the distal humerus and proximal ulna using 3D bone models constructed from the CT data and to compare them between normal cadavers and RA patients.

Materials and methods

We studied the elbow joints of 16 seropositive rheumatoid patients, who were scheduled for TEA (15 women and 1 man; age range, 48-81 years; mean age, 60.6 years) and 20 cadaveric dry bones (10 humeri and 10 ulnae) (Natural Bone; Sawbones [A Division of Pacific Research Laboratories], Vashon, WA). The inclusion criteria for RA patients included RA of grade III to V based on the radiographic criteria of Larsen et al,[10] severe disabling pain, limitation of elbow function, and no previous surgical treatment. Of the patients, 9 (56.2%) had Larsen grade III RA, 4 (25%) had Larsen grade IV RA, and 3 (18.8%) had Larsen grade V RA. The right elbow was affected in 10 patients and the left elbow in 6.

Image acquisition

Morphologic analysis of the medullary canal was performed by use of CT scans. Image data of the elbows from RA patients and cadavers were obtained with a helical CT system (Light Speed Ultra16; GE Medical Systems, Waukesha, WI). We used a sequence with 120 kV, 100 mA, a 300-mm field of view, and a thickness of 0.625 mm on a contiguous slice with a pixel size of 0.39 × 0.39 mm. During CT scanning, the elbow joint was maximally extended with the forearm in a neutral position. Scan data were saved in DICOM (Digital Imaging and Communications in Medicine) format.

Three-dimensional bone models and measurement

Contours and medullary structures of each bone were semiautomatically segmented from CT images by use of the Virtual Place-M software program (Medical Imaging Laboratory, Tokyo, Japan). This software generated 3D surface bone models via the marching cubes technique,[13] based on which we constructed bone models of each humerus and ulna. A threshold for constructing these models is an important parameter for determining their accuracy. In this study, we used 150 Hounsfield units as an optimal threshold value.[21] The contours of the medullary canal were extracted semiautomatically, and the visualization and measurement of the geometric shape and size of each bone were obtained by use of a visualization software program developed in our laboratory. The accuracy of this computer-based measurement was reported to be 0.4 mm.[17]

We resliced the 3D surface bone models of the medullary canal vertically along the longitudinal axis of each canal and evaluated the change in medullary shape of the reconstructed cross section of the humeral medullary canal, from the proximal margin of the olecranon fossa, and for the ulna, from the tip of the coronoid process, at intervals of 1 cm. Then, we calculated the area, as well as the anteroposterior and transverse diameters, of each cross-sectional slice of the medulla of the humerus and the ulna.

Statistical analysis

Mann-Whitney *U* tests were performed for statistical differences between normal controls and RA patients. A difference with $P < .05$ was considered significant. This statistical analysis was conducted with the Statcel2 statistical analysis software package for personal computers (OMS Publishing, Saitama, Japan).

Results

Morphology of humerus

The cross-sectional shape of the humerus changed from a V shape to an equilateral triangle and then to ovoid in both RA patients and cadavers (Figure 1, *A*). The cross-sectional area particularly decreased at 0 cm above the olecranon fossa compared with the cadavers ($P < .05$). It also tended to decrease at a distance of 1 cm (Figure 2, *A*). Whereas the mean anteroposterior diameter was not significantly different between RA patients and controls, the mean transverse diameter was significantly decreased at 0 and 1 cm in the RA patients as compared with the controls ($P < .05$), as shown in Figures 2, *B*, and 2, *C*. In RA patients and cadavers, the cross-sectional areas were approximately 100 mm^2 at 2 cm and 80 mm^2 at 3 to 10 cm and then they increased gradually at 11 cm. The mean anteroposterior diameters of the humerus tended to increase gradually toward the diaphysis, whereas the transverse diameters gradually decreased.

Morphology of ulna

For the ulna, the shape changed from ovoid to triangular (Figure 1, *B*), and the cross-sectional area decreased at 0 and 1 cm distal to the coronoid process in the RA patients ($P < .05$) (Figure 3, *A*). In the ulna, both the mean anteroposterior and transverse diameters were significantly decreased at 0 and 1 cm, respectively, in the RA patients compared with the controls ($P < .05$) (Figures 3, *B*, and 3, *C*). This discrepancy between RA patients and cadavers was produced by the morphologic changes observed around the trochlear notch of the ulna. In both RA patients and cadavers, the cross-sectional areas were approximately 50 mm^2 at 3 cm and 20 mm^2 at 7 cm to 14 cm. Both the mean anteroposterior and transverse diameters of the ulna tended to decrease gradually toward the diaphysis.

Discussion

TEA can preserve, or even improve, the range of motion of the joints, eliminate pain, and provide adequate stability to the arthritic joint. One major concern regarding TEA is loosening of the implants. Although improvement of surgical technique and prosthetic design has led to

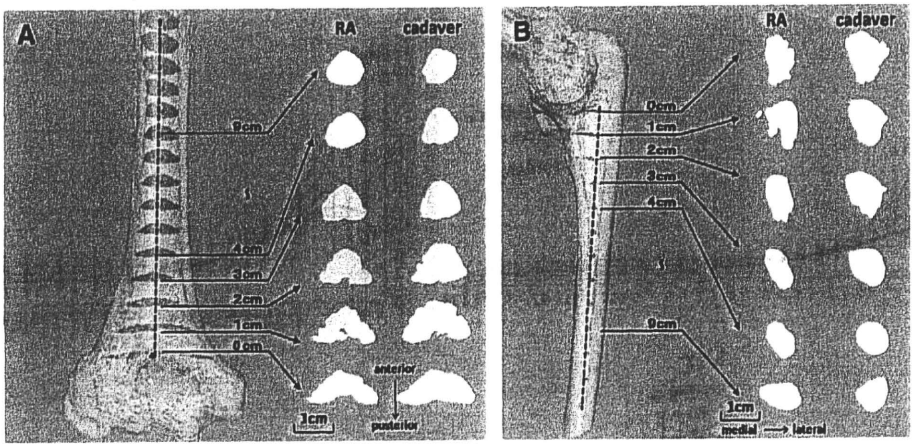

Figure 1 (A) Cross-sectional area of medullary canal of humerus. We evaluated the cross-sectional area from the proximal margin of the olecranon fossa at 1-cm intervals. The cross-sectional shape of the humerus changed from a V shape to an equilateral triangle and then to ovoid in both RA patients and cadavers. The cross-sectional area of RA has especially decreased at 0 cm above the olecranon fossa because of the morphologic change around the coronoid fossa, as compared with the cadavers ($P < .05$). (B) Cross-sectional area of medullary canal of ulna. The geometric shape of the cross-sectional area changed from ovoid to triangular. In the RA patients, the cross-sectional area decreased at 0 and 1 cm distal to the tip of the coronoid process because of the morphologic change around the trochlear notch of the ulna.

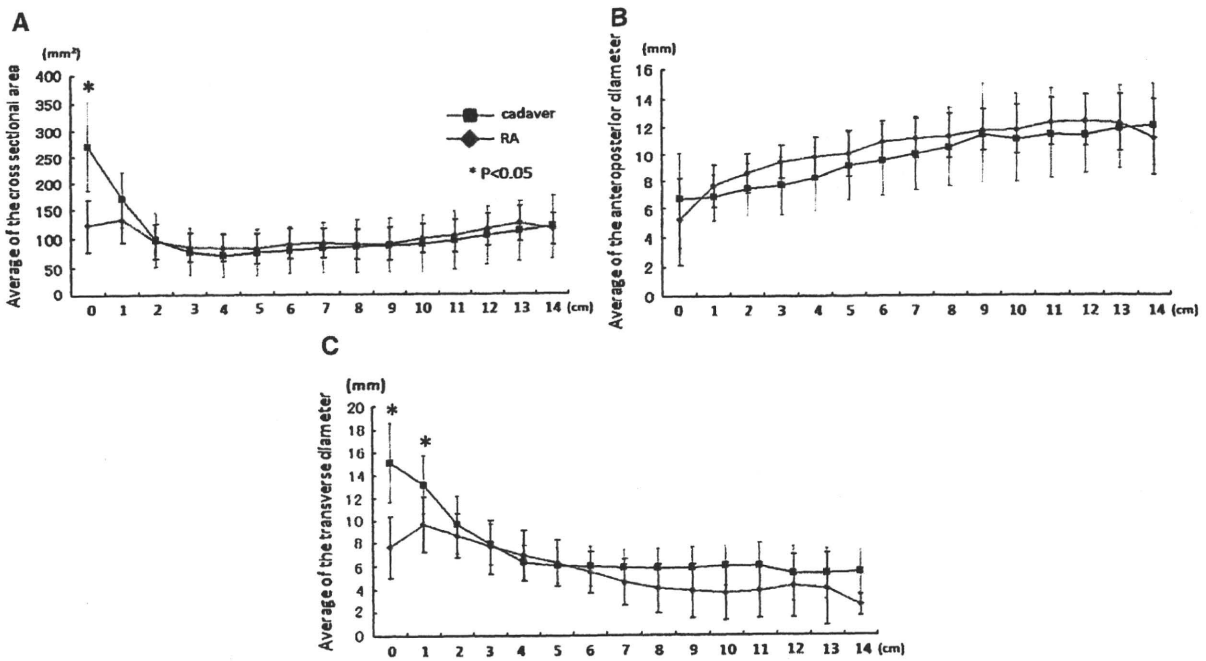

Figure 2 Measurement of medullary canal of humerus. (A) The mean cross-sectional area of the humerus is shown with SD error bars. *Asterisk*, A significant difference was found between the RA patients and cadavers ($P < .05$). (B) Mean anteroposterior diameters of cross section. (C) Mean transverse diameters of cross section.

increased longevity of TEA, the loosening rate is still higher when compared with total hip and knee arthroplasties.[5,6,8,18,19,23,26] In RA patients, van der Lugt et al[26,27] reported that the survival rate of the Souter-Strathclyde prosthesis, according to Kaplan-Meier analysis, was 77.4% after 10 years and 65.2% after 18 years. A high rate of aseptic loosening of the humeral component has been frequently described, whereas the success rate was found to be different among the types of TEA.[5,8,18,23,26] Although several authors postulate that the loosening was because of the micromovement, the reason for this phenomenon remains unclear.[2,24] Ikavalko et al[3,4] reported that the standard stem humeral component has better survivorship compared with the long-stemmed component.

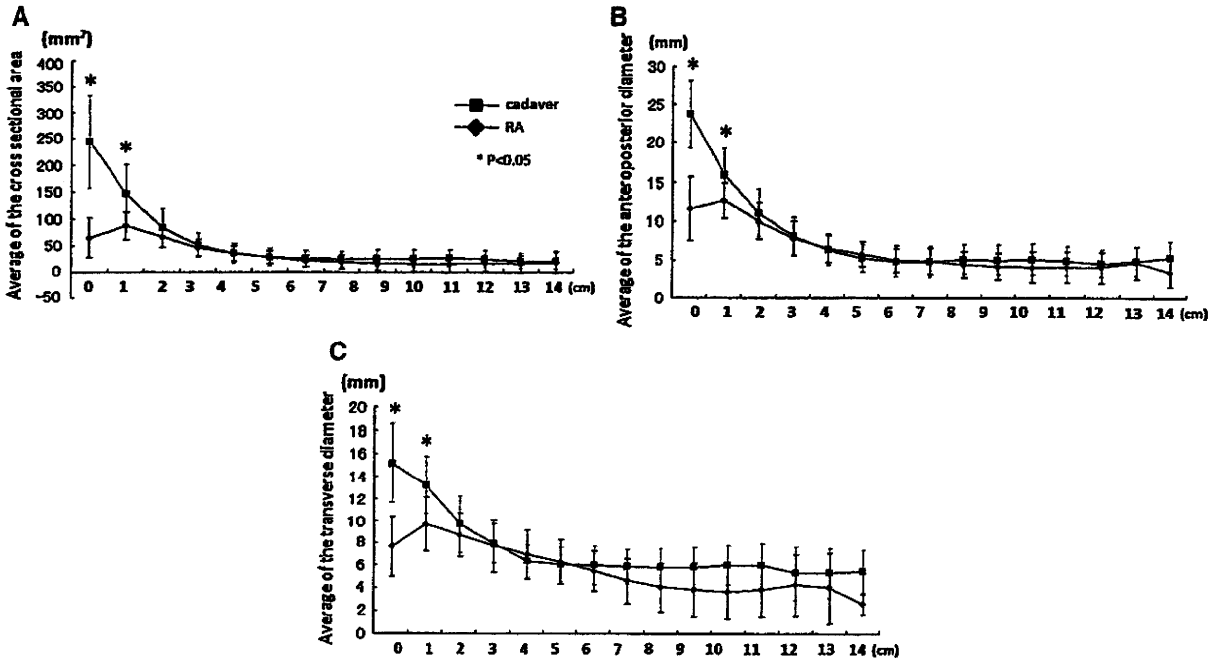

Figure 3 Measurement of medullary canal of ulna. (**A**) The mean cross-sectional area of the ulna is shown with SD error bars. *Asterisk*, A significant difference was found between the RA patients and cadavers ($P < .05$). (**B**) Mean anteroposterior diameters of cross section. (**C**) Mean transverse diameters of cross section.

We assumed that the morphologic change of periarticular inflammatory reaction from arthritis could possibly be one of the reasons for early aseptic loosening after TEA, as it can decrease the stability of the implant in regard to the bone. Therefore, it would be important to evaluate the morphologic change around the elbow joint in RA patients accurately. There have been several detailed studies of the geometry of the medullary canals based on radiographs.[7,11,20] However, it is quite difficult to quantify the extent of the bone loss correctly, based only on plane radiographs.

On the other hand, several authors believe that an anatomic, custom-designed femoral component of total hip arthroplasty is more likely to be effective than off-the-shelf components to achieve the optimal fit and fill the medullary canal.[14,15,28,29] The geometry of the medullary canals of the distal humerus and proximal ulna is considered important for the appropriate design of stems for the TEA prosthesis to increase its stability in the bone and decrease the rate of loosening. Our measurements were derived from 3D constructions of the medullary canal, based on the CT data obtained with a high-speed helical scanner. This allowed us to compare the morphology of the normal controls with the RA group accurately.

High loosening rates of the humeral component have been reported previously.[5,8,18,23,26] On the basis of the data obtained from this study, the anteroposterior diameters of the humerus have tended to increase toward the diaphysis whereas the transverse diameters have decreased (Figure 2, *B*). When considering the initial fixation of the press-fit uncemented stem of the humeral component in future prosthetic design, the width of the transverse diameter is considered more important than the anteroposterior diameter. Increasing the width of the transverse diameter of the intramedullary stem could increase the stability of the humeral component in the canal.

Several authors have noted that aseptic loosening and failure, because of loosening, occur more often with the ulnar component than with the humeral component and that the ulnar component is at high risk of loosening.[1,9,16,22,25] Furthermore, in RA patients, aseptic loosening of the ulnar component was found more often in uncemented ulnar components than in cemented ones. Our results showed that there is a significant morphologic change in the proximal ulnar medullary canal in the area from the coronoid process to 3 cm distally, where the stem of the prosthesis is expected to fit. This change in the morphology would make press fitting of the ulnar component into the canal quite difficult, even with an anatomically designed stem. We believe that the ulnar component would be better stabilized by a cement technique, especially in cases of severe morphologic change.

References

1. Brinkman JM, de Vos MJ, Eygendaal D. Failure mechanisms in uncemented Kudo type 5 elbow prosthesis in patients with rheumatoid arthritis: 7 of 49 ulnar components revised because of loosening after 2-10 years. Acta Orthop 2007;78:263-70.

2. Brunski BJ, Puelo DA, Nanci A. Biomaterials and biomechanics of oral and maxillofacial implants: current state and future developments. Int J Oral Maxillofac Implants 2000;15:15-46.
3. Ikavalko M, Belt EA, Kautiainen H, Lehto MU. Revisions for aseptic loosening in Souter-Strathclyde elbow arthroplasty: incidence of revisions of different components used in 522 consecutive cases. Acta Orthop Scand 2002;73:257-63.
4. Ikavalko M, Lehto MU, Repo A, Kautiainen H, Hamalainen M. The Souter-Strathclyde elbow arthroplasty. A clinical and radiological study of 525 consecutive cases. J Bone Joint Surg Br 2002;84:77-82.
5. Kasten MD, Skinner HB. Total elbow arthroplasty. An 18-year experience. Clin Orthop Relat Res 1993:177-88.
6. Khaw FM, Kirk LM, Gregg PJ. Survival analysis of cemented Press-Fit Condylar total knee arthroplasty. J Arthroplasty 2001;16:161-7.
7. Kitamura T, Hashimoto J, Murase T, Tomita T, Hattori T, Yoshikawa H, et al. Radiographic study of joint destruction patterns in the rheumatoid elbow. Clin Rheumatol 2007;26:515-9.
8. Kraay MJ, Figgie MP, Inglis AE, Wolfe SW, Ranawat CS. Primary semiconstrained total elbow arthroplasty. Survival analysis of 113 consecutive cases. J Bone Joint Surg Br 1994;76:636-40.
9. Landor I, Vavrik P, Jahoda D, Guttler K, Sosna A. Total elbow replacement with the Souter-Strathclyde prosthesis in rheumatoid arthritis. Long-term follow-up. J Bone Joint Surg Br 2006;88:1460-3.
10. Larsen A, Dale K, Eek M. Radiographic evaluation of rheumatoid arthritis and related conditions by standard reference films. Acta Radiol Diagn (Stockh) 1977;18:481-91.
11. Lehtinen JT, Kaarela K, Belt EA, Kauppi MJ, Skyttä E, Kuusela PP, et al. Radiographic joint space in rheumatoid elbow joints. A 15-year prospective follow-up study in 74 patients. Rheumatology (Oxford) 2001;40:1141-5.
12. Lehtinen JT, Kaarela K, Ikävalko M, Kauppi MJ, Belt EA, Kuusela PP, et al. Incidence of elbow involvement in rheumatoid arthritis. A 15 year endpoint study. J Rheumatol 2001;28:70-4.
13. Lorensen WE, Cline HE. Marching cubes: a high resolution 3-D surface construction algorithm. Computer Graphics 1987;21:163-9.
14. McCarthy JC, Bono JV, O'Donnell PJ. Custom and modular components in primary total hip replacement. Clin Orthop Relat Res 1997: 162-71.
15. Mulier JC, Mulier M, Brady LP, Steenhoudt H, Cauwe Y, Goossens M, et al. A new system to produce intraoperatively custom femoral prosthesis from measurements taken during the surgical procedure. Clin Orthop Relat Res 1989:97-112.
16. Potter D, Claydon P, Stanley D. Total elbow replacement using the Kudo prosthesis. Clinical and radiological review with five- to seven-year follow-up. J Bone Joint Surg Br 2003;85:354-7.
17. Robertson DD, Yuan J, Bigliani LU, Flatow EL, Yamaguchi K. Three-dimensional analysis of the proximal part of the humerus: relevance to arthroplasty. J Bone Joint Surg Am 2000;82:1594-602.
18. Rozing P. Souter-Strathclyde total elbow arthroplasty. J Bone Joint Surg Br 2000;82:1129-34.
19. Sathappan SS, Teicher ML, Capeci C, Yoon M, Wasserman BR, Jaffe WL. Clinical outcome of total hip arthroplasty using the normalized and proportionalized femoral stem with a minimum 20-year follow-up. J Arthroplasty 2007;22:356-62.
20. Stein H, Dickson RA, Bentley G. Rheumatoid arthritis of the elbow. Pattern of joint involvement, and results of synovectomy with excision of the radial head. Ann Rheum Dis 1975;34:403-8.
21. Sugano N, Sasama T, Sato Y, Nakajima Y, Nishii T, Yonenobu K, et al. Accuracy evaluation of surface-based registration methods in a computer navigation system for hip surgery performed through a posterolateral approach. Comput Aided Surg 2001;6:195-203.
22. Tanaka N, Kudo H, Iwano K, Sakahashi H, Sato E, Ishii S. Kudo total elbow arthroplasty in patients with rheumatoid arthritis: a long-term follow-up study. J Bone Joint Surg Am 2001;83:1506-13.
23. Trail IA, Nuttall D, Stanley JK. Survivorship and radiological analysis of the standard Souter-Strathclyde total elbow arthroplasty. J Bone Joint Surg Br 1999;81:80-4.
24. Valstar ER, Garling EH, Rozing PM. Micromotion of the Souter-Strathclyde total elbow prosthesis in patients with rheumatoid arthritis 21 elbows followed for 2 years. Acta Orthop Scand 2002; 73:264-72.
25. van der Heide HJ, de Vos MJ, Brinkman JM, Eygendaal D, van den Hoogen FH, de Waal Malefijt MC. Survivorship of the KUDO total elbow prosthesis-comparative study of cemented and uncemented ulnar components: 89 cases followed for an average of 6 years. Acta Orthop 2007;78:258-62.
26. van der Lugt JC, Geskus RB, Rozing PM. Primary Souter-Strathclyde total elbow prosthesis in rheumatoid arthritis. J Bone Joint Surg Am 2004;86:465-73.
27. van der Lugt JC, Rozing PM. Outcome of revision surgery for failed primary Souter-Strathclyde total elbow prosthesis. J Shoulder Elbow Surg 2006;15:208-14.
28. Wettstein M, Mouhsine E, Argenson JN, Rubin PJ, Aubaniac JM, Leyvraz PF. Three-dimensional computed cementless custom femoral stems in young patients: midterm followup. Clin Orthop Relat Res 2005:169-75.
29. Xenakis TA, Gelalis ID, Koukoubis TD, Soucacos PN, Vartziotis K, Kontoyiannis D, et al. Neglected congenital dislocation of the hip: role of computed tomography and computer-aided design for total hip arthroplasty. J Arthroplasty 1996;11:893-8.